
Politecnico di Torino

Master Course in Environmental and Land Engineering

Specialization in Climate Change

A.A 2023/2024

Master's Thesis:
# Beneficial aspects of climate change and the case of meltwater runoff

Relator: Stefania Tamea
Candidate: Aurora Sesto Ferreri

# SOMMARIO

**Abstract** ..... **5**
**Beneficial aspects of climate change** ..... **6**
**Increased Agricultural Productivity: Grape vines** ..... **7**
**Biodiversity Shifts** ..... **11**
**Effects on humans** ..... **16**
**Emerging opportunities in mountains** ..... **18**
**The Case of Meltwater Runoff** ..... **21**
Objective ..... 21
Materials and methods ..... 21
Catchments in Valle d'Aosta and Piedmont with SAGA tools in QGIS ..... 22
Volume of water from glacier melt within these catchments ..... 24
How different climate scenarios (RCPs) might impact glacier melt and runoff in the future projections and compared to past rate of melting water ..... 25
Sitografia ..... 48
Bibliografia ..... 48

# Abstract

This thesis delves into the often-overlooked beneficial aspects of climate change, examining several key phenomena that have the potential to yield positive outcomes amidst the broader challenges posed by global warming. This thesis examines various positive dimensions of climate change identified through the analysis of scientific literature. Key areas of focus include increased agricultural productivity, biodiversity shifts, effects on human's bodies, and emerging opportunities in mountain regions.

The first part of the thesis synthesizes findings on agricultural productivity, revealing how changing climatic conditions have facilitated enhanced crop yields in certain regions. Biodiversity shifts are explored, noting both challenges and opportunities arising from species adaptation and migration patterns in response to altered climates. Effects on humans' bodies like better competitors' performance and emerging opportunities in mountains such as increasing of tourism, and the rising of the tree line.

In the second part, the thesis delves into the critical issue of water resources, with a specific focus on meltwater runoff dynamics under changing climatic scenarios. The case of meltwater runoff is examined in depth, evaluating interactions, the dynamics of ice mass melt, and projections of future water availability. Comparisons between past trends and future projections under different Representative Concentration Pathways (RCPs), specifically RCP 2.6 and RCP 8.5, illuminate varying trajectories of water resource availability in the coming decades.

Overall, this thesis contributes a nuanced perspective on climate change impacts by highlighting not only challenges but also potential benefits and opportunities across agricultural productivity, biodiversity, human societies, and water resources. This holistic view underscores the importance of adaptive strategies and informed policymaking in mitigating the negative consequences while harnessing potential benefits of a changing climate.

By shedding light on these beneficial aspects of climate change, this thesis aims to broaden the discourse surrounding climate change mitigation and adaptation strategies. While acknowledging the overarching negative impacts of global warming, understanding and leveraging these positive outcomes can inform more nuanced and comprehensive approaches to addressing the complex challenges posed by climate change.

# Beneficial aspects of climate change

In this thesis, we conducted a literature review to extract the positive aspects of climate change and present them. It is unfortunately common to focus extensively on the negative aspects and anticipate what will happen, but according to our principles, it is more important to seize upon what is positive and strive to enhance and harness it for the benefit of future generations inhabiting planet Earth. The positive aspects studied are focused on the Italian territory, with a couple of articles also addressing biodiversity in Europe.

Numerous scientific sources highlight certain potential positive aspects of climate change:

Increased Agricultural Productivity: Some studies suggest that in certain regions of Italy climate conditions could enhance the productivity in grape vines [1].

Biodiversity Shifts: Climate change could lead to shifts in species distributions, potentially increasing species richness in certain areas of Italy and Europe as new species migrate into these regions [2]

Effects on humans: The analysis of the mechanism shows that the increase in ambient temperature can enhance competitors' performances by expanding the air and thereby reducing air resistance for competitors or equipment thrown in these events [3]

Emerging opportunities in mountains: With increasing global temperatures, vegetation belts will shift to higher altitudes and move northward [4]

While these potential benefits exist, it is crucial to note that they come with significant caveats and are often overshadowed by the numerous negative impacts of climate change. Moreover, the long-term consequences of these changes are uncertain and may vary widely depending on regional and global responses to climate change.

By focusing on these potential benefits, we aim to underscore the importance of understanding both sides of the climate change equation and using this knowledge to inform strategies that maximize positive outcomes while mitigating the negative impacts for future generations.

## Materials and methods

Approximately 30 articles from various scientific sources such as Web of Science, Scopus, Research Gate, Science Direct, and journals like Nature were analyzed.

These articles cover a timeframe ranging from 2008 to the recent year of 2023. The keywords used to identify the most relevant articles include "positive climate change," "land productivity," "tree of life", "human effects" and "biodiversity."

## Increased Agricultural Productivity: Grape vines

Viticulture is deeply intertwined with weather and climate conditions. Across centuries, winegrowers have adapted their practices to thrive in diverse geographical regions. However, this delicate balance faces challenges from climate change. Studies have assessed the vulnerability of crops to climate change. Research underscores how increasing temperatures and shifting rainfall patterns impact grape growth. Temperature notably influences phenology, potentially advancing growth stages and shortening the growing season, affecting harvest quality. Earlier budburst due to warmer temperatures increases susceptibility to frost events, while altered precipitation patterns can elevate pest and disease risks. [1]

Significant shifts in wine-growing suitability are anticipated in traditional regions like Italy, potentially leading to decreased production. Italy, a global leader in wine production, saw its wine exports valued at 7 billion euros in 2021, marking a 12.4% increase from 2020 and a 51.5% increase from 2012. With nearly 10% of the world's wine production area, Italy ranked as the top wine producer in 2022 (49.8 million hectoliters), followed by France (45.6 Mio hl) and Spain (35.7 Mio hl). [1]

Data used in this study was collected by the Italian National Institute of Statistics (ISTAT) that collects yearly data on grape yields and vineyard acreage for the wine industry, spanning from 1980 onwards. However, the spatial aggregation of this data varies over different time periods: from 1980 to 1993 and 2006 to 2019, data are at the provincial level (NUTS3), from 1994 to 2000 at the regional level (NUTS2), and from 2000 to 2005 at the national level (NUTS0). To standardize the data, a method was applied to aggregate NUTS3 data to NUTS2 level where necessary, ensuring a comprehensive time series from 1980 to 2000 and 2006 to 2019. [1]

The choice of NUTS2 aggregation is optimal due to its balance between capturing long-term trends and accounting for regional viticultural policies. This approach aligns with the study's aim to analyze grape productivity (grape yield per hectare) independent of changes in vineyard size. It covers a 35-year period and effectively captures the spatial variability of grape productivity across Italy's wine-producing regions. [1]

This study presents an overview of bioclimatic indices used to assess the impact of climate on viticulture, particularly focusing on Italy. Following OIV recommendations, five temperature-based indices and two precipitation-based

indices are selected:

→ Mean Temperature During Vegetation Period (TmVeg)
→ Heliothermic Huglin Index (HI)
→ Winkler Degree Days (WI)
→ Biologically Effective Degree Days (BEDD)
→ Cool Night Index (CNI)

The two precipitation-based indices are:

→ Growing Season Precipitation Index (GSP)
→ Spring Rain Index (SprR)

[1]

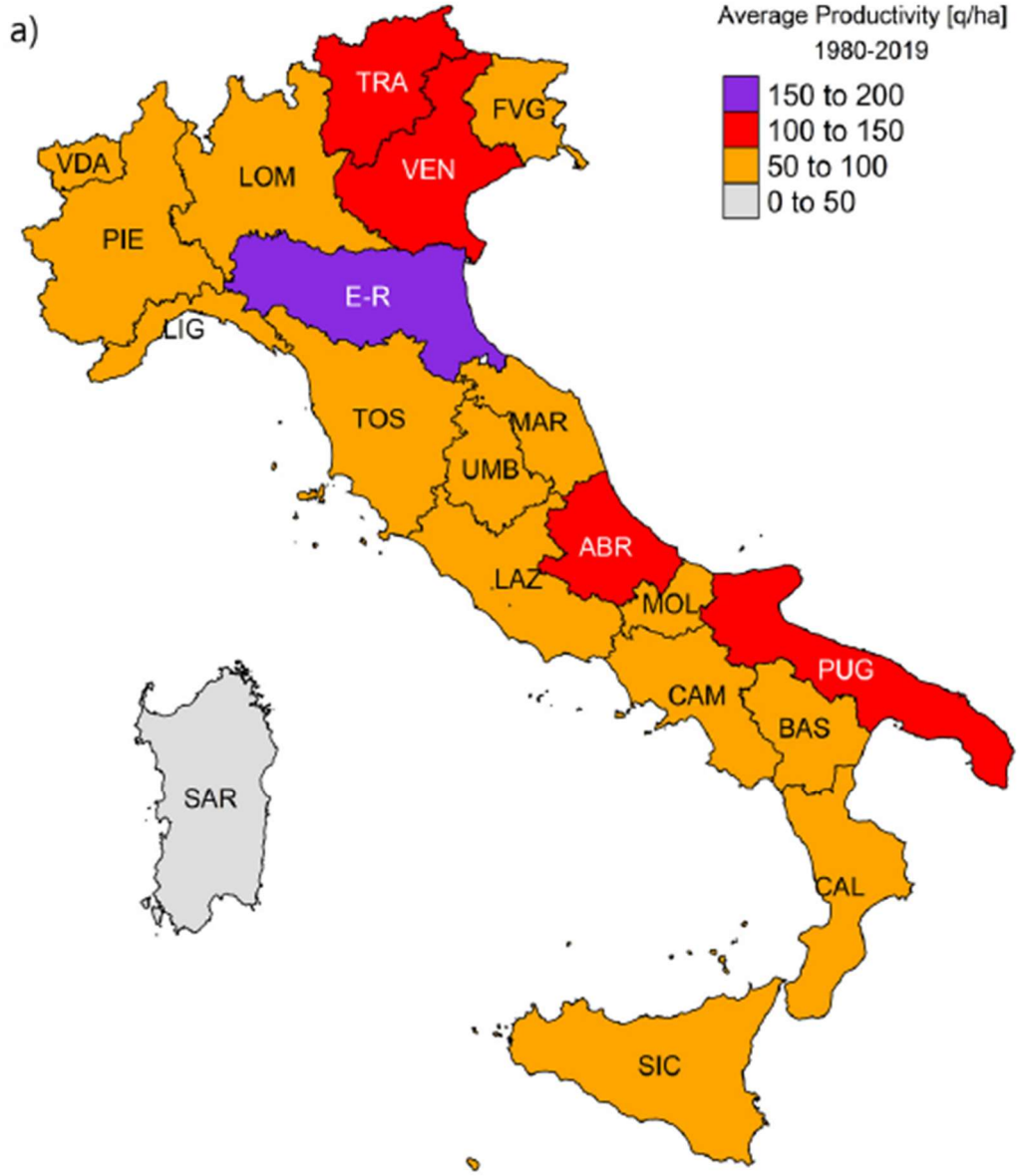

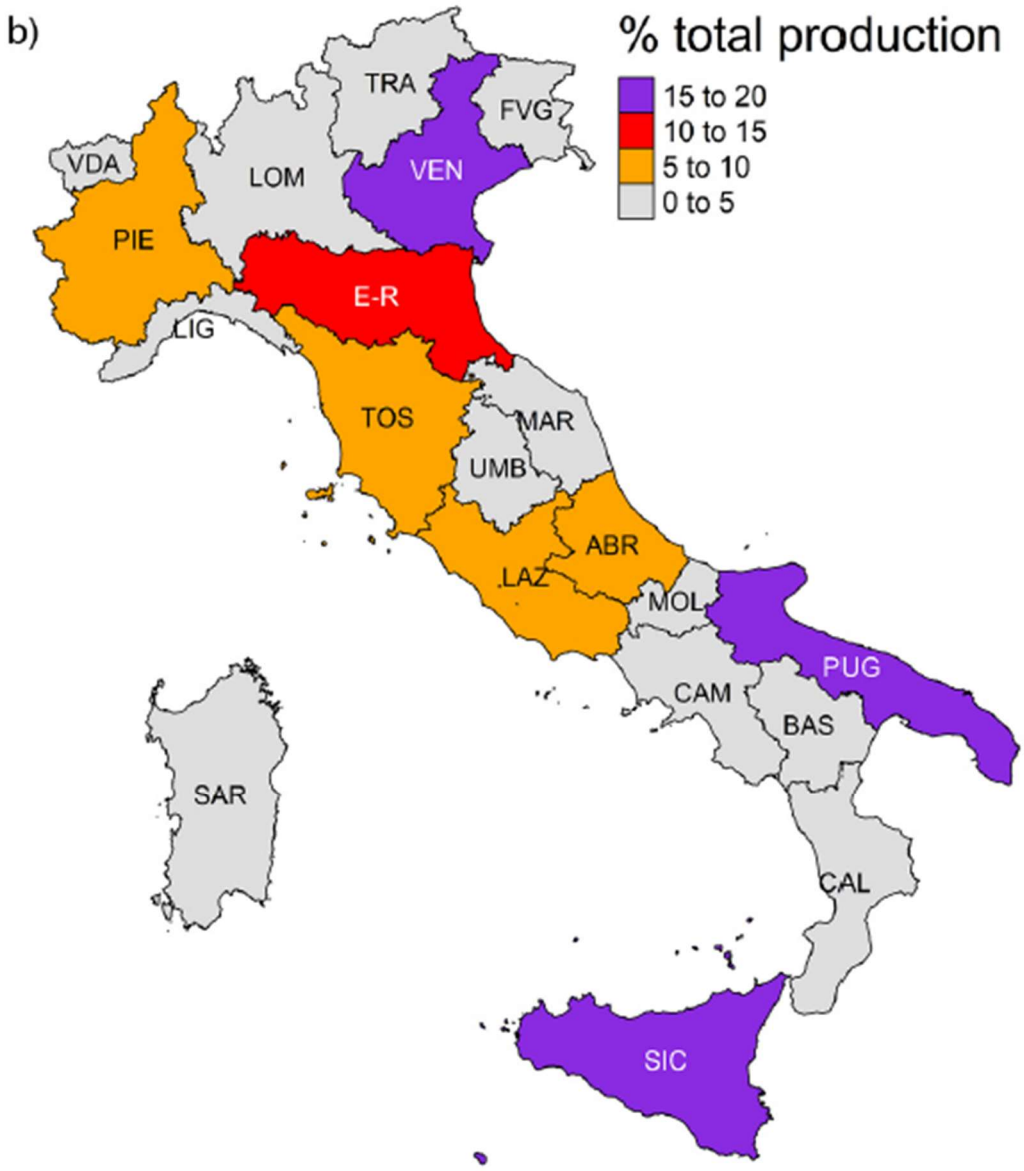


*Figure 1: Map of Italy showing a) yearly average productivity (q/ha) in the period 1980–2019 and b) contribution to the national total production in each region in percentage.* [1]

The time series analysis of bioclimatic indices reveals that temperature-based indices are unfavorable for grapevine growth in three regions—Friuli Venezia Giulia (FVG), Trentino-Alto Adige (TRA), and Valle d'Aosta (VDA)—which collectively contribute less than 5% to Italy's total production. Specifically, these regions exhibit "too-cold" BEDD values, while "too-cold" HI, WI, and TmVeg values are noted in TRA and VDA *(Figure 1).* Despite these unfavorable conditions, there is no significant decrease in productivity observed. This suggests a high level of local adaptation to adverse climatic conditions and indicates the necessity of adjusting the existing thresholds for Alpine regions like FVG, TRA, and VDA. Additionally, "very cool nights" are common in central and northern Italy, whereas warm nights are more prevalent in southern regions such as Puglia (PUG), Sardegna (SAR), and Sicilia (SIC). However, no statistically significant relationship between productivity and CNI or precipitation-based indices was

found.
This study aims to establish a direct statistical link between bioclimatic indices commonly used in viticulture and grape productivity in Italy, using 35 years of data from ISTAT and the E-OBS climate dataset. The research employs single and multi-regressive approaches to analyze the impact of climate on grape productivity at the regional level (NUTS2).

The single-regression analysis of raw data reveals mostly positive correlations between productivity and temperature-based indices, indicating adaptation to increased temperatures over time. Notable regions such as Veneto (VEN), Puglia (PUG), and Emilia-Romagna (E-R) show that a single index can explain up to 35% of productivity variance. Negative correlations with precipitation-based indices in Piemonte (PIE) suggest that excessive rain increases the risk of fungal diseases, negatively affecting the harvest.

Long-term climate trends impact productivity more than inter-annual variability. The multi-regressive model, combining temperature and precipitation indices, effectively predicts productivity across most regions, particularly for long-term trends. This model explains up to 54% of productivity variability on an inter-annual scale in Trentino Alto Adige (TRA) and up to 52% in Veneto (VEN) and Puglia (PUG) for long-term trends.

Unexplained variance may be due to factors other than climate, such as viticultural practices, soil types, grape varieties, policies, and market conditions. The study emphasizes the need for high-quality data and the involvement of local businesses and stakeholders to better address the challenges posed by climate variability. [1]

The study's findings indicate a potential positive aspect of climate change for viticulture in Italy. The developed predictive models, which explain up to 52% of the historical harvest variability, could become valuable tools for estimating future changes in productivity. This suggests that with appropriate adaptation strategies and predictive tools, wine grape production could be better managed in the face of climate change. Furthermore, the methodology can be applied to other regions, potentially benefiting the global viticulture industry by providing insights into how to optimize production under changing climatic conditions. Thus, the development of these models and the potential for improved management strategies represent a positive outcome derived from studying the impacts of climate change on viticulture.

Other study suggest to develop innovative agronomic practices to counteract the various negative effects of extreme climatic events by equipping vineyards with effective, reliable, and economically sustainable multifunctional systems. Specifically, a multifunctional irrigation system can be used to mitigate the risk of extreme weather events while simultaneously improving the quality and quantity of grape production and reducing interannual variability by providing optimized water

nutrition for the plants. [5]

In a vineyard located south of Lake Garda (Northern Italy), a multifunctional irrigation system equipped with drippers and mini-sprinklers (the latter used to protect against both late spring frost and high summer temperatures) was evaluated. The results obtained for the 2020-2021 growing season showed that optimized drip irrigation reduced water consumption without affecting grape yield, both in terms of quantity and quality. Frost protection operated by mini-sprinklers increased the air temperature at bud level by about 1 °C, suggesting a positive effect on plant production. Additionally, in 2020, must quality was positively affected by summer sprinkler irrigation, increasing malic acid levels and titratable acidity by over 0.7 g L^-1 while lowering total soluble solids. Further activities in the 2022 season aim to better assess the water use efficiency of this promising multifunctional system. [5]

The study on multifunctional irrigation systems aimed at improving vineyard resilience to climate change demonstrated that optimized irrigation can significantly reduce water usage without affecting grape yield or quality. These systems effectively manage water stress, late spring frosts, and high summer temperatures by using monitoring systems to assess crop-soil water status. [5]

Key findings include:

- The method of distributing water over time in sprinkler systems was more crucial for temperature reduction than the flow rate.
- Despite a mild water deficit during the study period, there was a trend of higher grape production due to evaporative cooling irrigation during thermal stress events.
- Sprinkler irrigation slightly improved bud fertility and positively impacted grape quality by increasing malic acid and titratable acidity levels.
- The results suggested no significant differences in grape quality based on the type of irrigation system used.

The research will continue into the 2022 season to further explore vine responses to water scarcity under different irrigation practices. [5]

# Biodiversity Shifts

Climate change is anticipated to significantly impact species diversity across Europe, particularly affecting plants, birds, and mammals.This study examines the projected effects of climate change on the diversity of plant, bird, and mammal species in Europe. It predicts that climate change will increase species vulnerability, potentially resulting in disproportionate effects on evolutionary history. However, despite a non-random distribution of vulnerable species across phylogenetic trees, the loss of evolutionary history does not appear to exceed

expectations based on models of random extinctions. Reductions in phylogenetic diversity will be more pronounced in Southern Europe, while gains are expected in high latitude or altitude regions. Nevertheless, these gains will not offset losses, leading to a trend towards homogenization of the tree of life across the continent. [2]

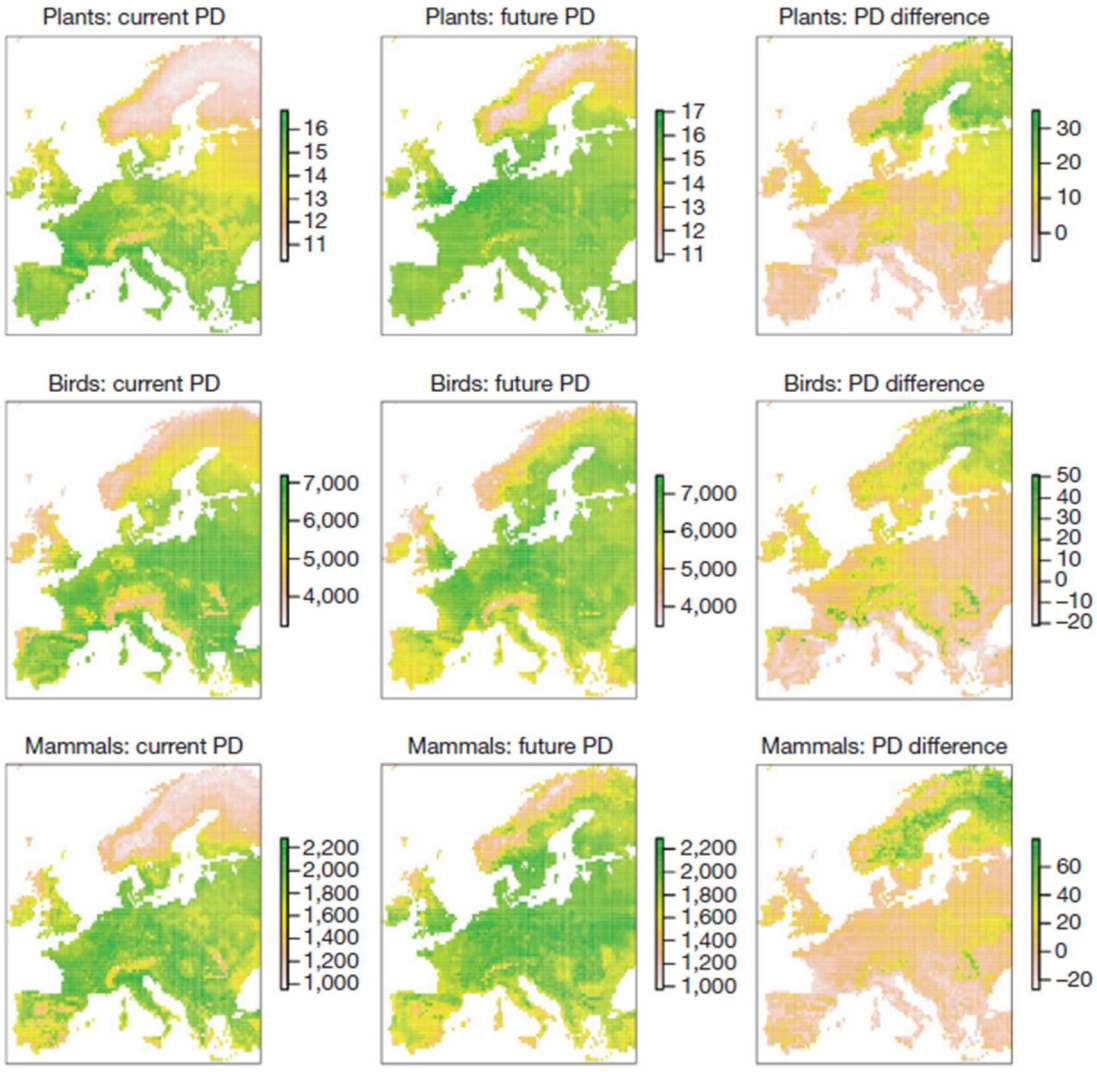


*Figure 2: Map of current and future phylogenetic diversities (A1FI scenario for 2080) and their relative differences for the three species groups. Maps represent average phylogenetic diversity (PD; colour scale) across the sample of 100 phylogenetic trees used for each study group.*

The IUCN (International Union for Conservation of Nature) Red List highlights selective extinction risks among amphibians, birds, and mammals, varying significantly within their respective families and orders. Historical fossil evidence indicates phylogenetically clustered extinctions, contrasting with earlier mass extinction events that were less selective. Our projections foresee no major drop in overall phylogenetic diversity but anticipate significant spatial reorganization of Europe's tree of life. This restructuring will lead to increased homogenization of phylogenetic diversity as species shift towards higher latitudes and elevations. [2]

Some study has investigated the shifts in breeding bird range margins in Great

Britain. New methodological approaches using standardized biological monitoring data offer robust opportunities to examine these patterns. It focus on north-south and elevational gradients, given the significant north-south temperature gradient in Great Britain compared to the east-west gradient. [6]

Using standardized bird abundance monitoring data from 1994 to 2009 in Great Britain, we empirically quantify range shifts while explicitly accounting for detection probability variation. We assess whether the magnitude of range margin shifts differs between trailing and leading range edges, as well as the species' range centers. Additionally, we examine whether the rate of change matches expectations based on warming degrees, as any lag in biotic response could indicate species' limitations in responding to rapid climate change.This study thus synthesizes the short-term impacts of recent warming on the spatial extent and abundance of species experiencing significant climate change. [6]

These results show that bird species in Great Britain have shifted their northernmost distribution points poleward by an average of 3.3 km per year, which is greater than shifts reported in other avian studies and the rate of community composition change across Europe. This standardized approach accounts for potential methodological biases and indicates that latitudinal shifts at the northern limits are greater than those at central and southern limits. Although our data is from part of each species' geographical range, the results are consistent whether analyzing the mean shift across species or within individual species' ranges. [6]

The leading edge of bird distributions has responded more to warming than the trailing edge, similar to patterns observed in terrestrial ectotherms where thermal tolerance primarily affects the leading edge. Warming may reduce cold limits at the leading edge, while biotic interactions at the trailing edge respond over longer timescales, especially in island contexts like the UK. This results in an average geographical range expansion of 15 km over 15 years, despite considerable interspecies variation. [6]

Short-term responses, like expanding ranges and stable populations, contrast with models projecting range contractions. This discrepancy could stem from focusing on species benefiting from climate change, which is unlikely based on other studies. Methodological biases in data collection are possible but do not appear to affect our conclusions. Other factors, such as land use changes, may also drive range extents, but most species do show a leading edge shift due to warming.
Contrasting climate change effects on species may manifest over different timescales. Immediate impacts at the leading edge from temperature increases and longer-term biotic interactions at the trailing edge require extended observation periods. Thus, despite no current range contraction, climate change impacts on biodiversity are significant due to projected future effects. Models predicting range shifts should be validated with recent trends and future projections should consider spatial heterogeneity in climate-distribution relationships. [6]

Ultimately, while short-term observations show expansions rather than contractions, long-term monitoring is essential to understand and attribute future biodiversity impacts due to climate change. Validating model predictions with empirical evidence will be a key challenge for ecologists.

Focusing on the Mediterranean area we have fund a study that examines the impact of climate change on Mediterranean gilthead seabream aquaculture using physiological modeling and two global climate change scenarios. The scenarios assess moderate and severe climate change effects on key aquaculture production indices across coastal Mediterranean regions over two-year farming cycles starting in 2021 (reference period), 2051 (mid-term), and 2091 (long-term). [7]

Key findings include:

- Time to market size: Climate change generally reduces the time to reach market size from 450 days by up to 36%.
- Feed conversion ratio: While it remains relatively stable at market size, it can increase by up to 10% over the two-year period due to faster growth in warmer waters.
- Fish weight: Fish achieve greater weights over the two-year cycle in warmer conditions.
- Temperature stress: The number of days with sea temperatures at or above 28°C, where seabream experiences stress, is tracked.

The outlook is generally positive in the mid-term but shows negative trends in the long-term, particularly affecting the most productive regions: Levantine, Aegean, Adriatic seas, and coastal Tunisia. Geospatially referenced simulation results are provided for specific regional analysis. [7]

This study reveals that climate change will significantly impact Mediterranean gilthead seabream aquaculture, particularly in the most productive regions today. Although warming generally shortens the time-to-market and results in larger fish sizes if the rearing time is fixed, extreme temperatures in some areas cause stress, reducing growth and increasing disease susceptibility. Adapting to climate change is essential for sustainable aquaculture development in the Mediterranean. Potential strategies include switching to more temperature-tolerant species, using engineered seabream stocks, adjusting stocking times to reduce exposure to warm days, and relocating aquaculture to more suitable areas like the western Mediterranean. Implementing timely and appropriate measures to mitigate and adapt to these changes is crucial for maintaining socio-ecological systems in the region. [7]

We have new species in the north of Italy:

→ the European bee-eater, which typically nests at latitudes reaching the 21°C isotherm in July (Cramp, 1985), has recently begun expanding into northern

Italy. This species, which remains gregarious throughout the year, is a summer visitor and breeder in Europe. In 2017, a small colony of 4-5 pairs was discovered in a mountainous area at around 1,250 meters above sea level in the western Alps. This finding demonstrates not only a latitudinal expansion but also an altitudinal one. [8]

→ Trithemis annulata, previously confined to southern Italy for over 150 years, has expanded its range over the last four decades, now inhabiting several alpine valleys. A comprehensive dataset of 2,557 geographical distribution points from 1825 to 2023 was used to analyze the expansion of T. annulata and the climatic conditions influencing its current and future distribution. Over 43 years, the species extended its northern range margin at about 12 km/year, accelerating to 34 km/year upon reaching the Po Plain. Despite this, its northward shift lagged behind the warming climate, estimated at 28 km/year. The suitable area for T. annulata in Italy is expected to grow significantly in the future. Notably, no consistent upward shift was observed. Human-induced climate warming has led to a substantial expansion of T. annulata's distribution, with northern populations now in Alpine valleys, potentially paving the way for its spread into central Europe. This analysis traces the northward expansion of Trithemis annulata in Italy, from its origins in the southwest to its arrival in South Tyrol by 2023. Over 43 years, T. annulata's northern range margin advanced at an average of 12 km/year, accelerating to 34 km/year in northern Italy over the last 7 years. This rapid expansion highlights the species' strong dispersal capability and adaptability to changing climatic conditions. Despite its success, T. annulata has struggled to keep pace with the northward shift of climate variables caused by human activity. As it continues to expand, T. annulata will colonize new freshwater habitats and compete with native and introduced species. This case exemplifies the importance of understanding species dispersal dynamics in a rapidly changing world. [9]

Some study investigates whether species richness can help stabilize plant productivity under warming conditions through compensatory responses in root biomass and functional traits. Using three herbaceous species, the researchers created plant communities in monocultures and two- and three-species assemblages, grown under current climate conditions, moderate warming, and severe warming. Mixed-linear models were used to analyze the impact of species richness and warming on plant productivity, species interaction, and root functional traits. [10]

The results showed that warming reduced both above- and below-ground productivity and changed the biodiversity-productivity relationship from negative to positive. Productivity declines were less severe in species-rich combinations. Warming reduced interspecific competition below-ground by decreasing the root biomass of strong competitors, allowing weaker competitors to grow more. This indicates that warming can promote compensatory responses in herbaceous root productivity, highlighting the importance of plant functional diversity in maintaining ecosystem functioning under climate change. [10]

Warming reduces below-ground interspecific competition by decreasing functional differences in root architecture between strongly competitive and less competitive species. These changes in species interactions can compensate for the negative effects of warming on productivity and mediate the impact of warming on the biodiversity-productivity relationship. The reduction of below-ground interspecific competition is particularly evident in highly diverse plant communities, where warming favors weaker competitors by limiting the root growth of stronger competitors. [10]

Theoretical studies have emphasized the role of species interactions in both biodiversity-productivity and biodiversity-stability relationships. This study provides empirical evidence that warming reduces below-ground competition through species-specific changes in root architecture, and that this reduction has compensatory effects on productivity, potentially stabilizing ecosystem functioning. [10]

## Effects on humans

Understanding both the positive and negative impacts of climate change is crucial for assessing and adapting to its effects. While climate warming is generally seen as having negative impacts, it can also positively affect human performance in anaerobic sports. In this it was analysed global weather and athlete performance data, it has been found that world-class athletes' performances in events like sprints, jumps, and throws improve with rising temperatures. For example, the 100m sprint time improves by 0.26 seconds as the temperature increases from 11.8°C to 36.4°C. [3]

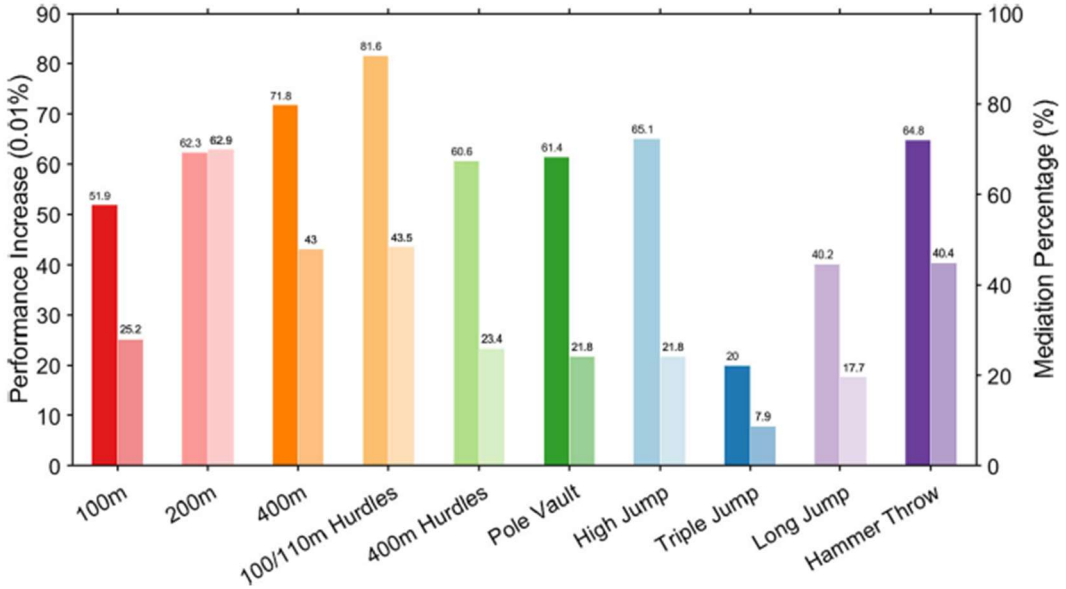


*Figure 3: Left bar for each event: percentage of performance improvement associated with 100 hPa decrease in ambient atmosphere pressure (unit: 0.01%). Right bar for each event: the proportion of the impacts of the ambient temperature rise on competitors' performance improvement that is taking effect through expanding the air and reducing air resistance to competitors or throwing implements (unit: 1.0%).* [3]

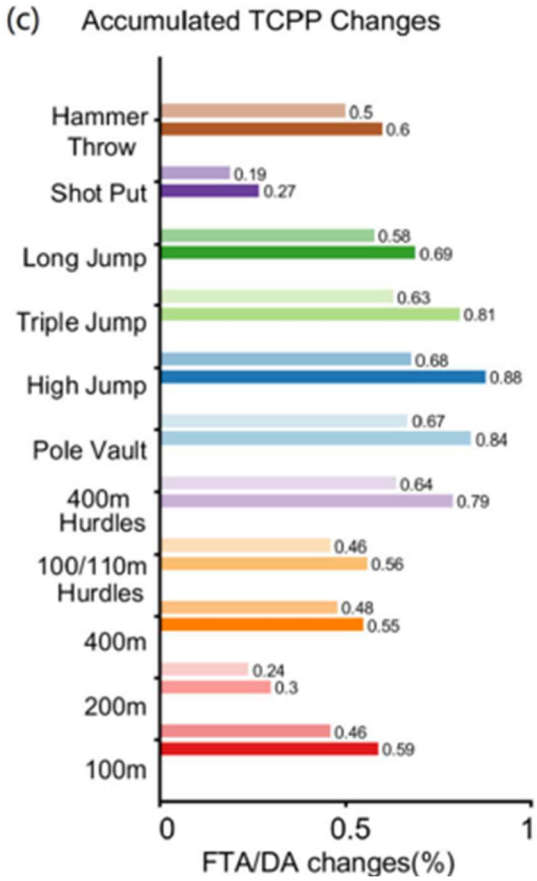


*Figure 4: Global TCPP changes of athletics anaerobic events due to warming climate. Global mixed-sex TCPP changes of the other 10 athletics events based on CMIP6 historical (1979–2014) climate simulations and future (2015–2100) projections under the scenario of SSP585. The TCPP changes are shown as the anomaly percentage to those during 2019–2021 and the results for 200 m, 400 m, 400m hurdles and 110/ 100m hurdles are reversed for visual purpose. c TCPP improvements (percentage) over 2014–2100 and 1979–2100 under SSP585 for the 11 events shown in Panel (a) and (b). The upper and lower bars for each event denote the improvement during 2014–2100 and 1979–2100, respectively. The TCPP changes during 1979–2014 are based on CMIP6 historical climate simulations.* [3]

Projections using the Coupled Model Intercomparison Project Phase 6 datasets indicate that global warming could enhance athletes' performances in most Olympic anaerobic events by 0.27%-0.88% under high-emission scenarios and 0.14%-0.48% under medium-emission scenarios from 1979 to 2100. Specifically, the 100m sprint could see improvements of 0.59% (0.063 seconds) and 0.32% (0.034 seconds) under high and medium emissions, respectively. The primary mechanism behind this improvement is the reduced air resistance caused by the expansion of the air in a warmer atmosphere, which benefits athletes in sprints, hurdles, jumps, and throwing events. This thermodynamic process is as significant as physiological factors in enhancing performance. [3]

## Emerging opportunities in mountains

Changing climatic conditions, such as temperature and precipitation patterns, along with other global changes, have heightened the vulnerability of mountain communities to various natural and socioeconomic risks. These changes pose significant environmental and developmental threats while also creating opportunities for sustainable development in mountain regions. Key opportunities include biodiversity conservation, high-value niche products like eco-tourism, hydro-energy, carbon trading, ecosystem service compensation, and the cultivation of high-value fruits, flowers, vegetables, and medicinal plants. Due to terrain and climate constraints, subsistence agriculture remains the primary livelihood for mountain communities. However, tourism has emerged as a significant livelihood option in both developed and developing mountain areas. It is now a major source of employment and foreign exchange, potentially reducing rural outmigration of educated and entrepreneurial individuals. Additionally, rising temperatures are making mountain destinations in subtropical and tropical regions more attractive to visitors, especially during summer months. [4]

Mountain systems, which contain nearly 50% of the world's biodiversity hotspots, support half of the planet's biological diversity and genetic resources, including many rare species. As global temperatures rise, vegetation belts are expected to shift to higher elevations and move northward in the northern hemisphere. These changes will likely alter the composition, structure, and distribution of biological resources. This shift creates opportunities for the conservation and sustainable development of high mountain ecosystems. Consequently, mountain ecosystems could provide essential protection for various species that might otherwise face extinction in lowland areas. [4]

The insurance argument emphasizes the importance of functional trait diversity in organisms, suggesting it may be more beneficial than mere taxonomic diversity. For example, a diverse range of plant architectures, especially below ground, can enhance resistance to disturbance and erosion. Thus, fewer but functionally diverse species might offer more benefits than many functionally similar ones. However, the specific traits that matter under extreme conditions are often unknown and may be hidden or only become evident under certain circumstances. Despite limited concrete evidence, the diversity of taxa acts as a safeguard against losing potential benefits. [11]

Slope stability is a critical issue in mountainous regions, as secure slopes depend on robust plant cover to prevent erosion. Research indicates that morphologically and phenologically diverse taxa are more likely to provide complete ground cover year-round, unlike a depleted set of taxa that may leave the ground exposed at times. Different species also respond variably to disturbances like grazing and trampling, depending on moisture conditions and substrate nature. Since these impacts are

unpredictable, a diverse set of taxa is more likely to maintain essential plant cover in mountain terrains. Single interventions, like fertilizer application or introducing new domestic animals, may cause certain species to fail, leading to erosion or landslides. Shrub encroachment into pastures can also alter slope stability through water infiltration. [11]

Other script has studied the dendroclimatic response of Pinus heldreichii across a broad elevation range (from 882 to 2143 m a.s.l.) in the southern Italian Apennines, hypothesizing a non-linear relationship between wood growth and air temperature along this gradient. Over three years (2012–2015), we collected wood cores from 214 pine trees at 24 sites, analyzing tree-ring data and genetic factors to understand growth acclimation. [12]

This analysis explores the influence of bell-shaped bioclimatic niches on a metapopulation of open-grown Pinus heldreichii across a wide elevation gradient in the Southern Italian Apennines. Despite no genetic structure detected across elevations, mean annual temperature and topographical aspect emerged as primary predictors of annual tree-ring variability along the gradient. The findings indicate contrasting responses to monthly air temperatures between low mountain and subalpine pines, leading to diminished differences in basal area increment (BAI) along the elevation gradient. [12]
Pines at higher elevations exhibited BAI comparable to those at lower elevations, benefitting from warmer air temperatures in early summer and previous autumn, consistent with climate change scenarios without drought stress. Conversely, pines at lower elevations showed a positive response to April temperatures, potentially counterbalancing the negative impact of increasing temperatures during other seasons.

This study underscores the high resistance and acclimation capability of Mediterranean elevation gradients to changing climatic conditions, suggesting low vulnerability and significant potential for carbon storage in these ecosystems in the future. It’s been identified average June air temperature as a critical factor influencing tree growth, revealing a bell-shaped thermal niche curve that peaks around 13–14 °C. This turning point aligns with global studies identifying optimal air temperatures for tree growth in cold climates. Moreover, it suggests that even species within small geographical ranges can adapt their climatic responses between different bioclimatic zones within their environmental niche, highlighting the resilience of old-growth forest stands. [12]

Here summarized the key findings of the study:
Increased tree productivity at higher elevations: Trees growing in the upper subalpine zones have achieved stem growth comparable to that of lower-elevation trees, thanks to warmer air temperatures during early summer and the preceding autumn. This indicates that trees in subalpine areas can benefit from higher temperatures associated with climate change.

High resistance and acclimation capability: The positive response to April temperatures at lower elevations can counterbalance the negative impact of increasing air temperatures during other seasons. This adaptability suggests that trees of this species have low vulnerability to changing climatic conditions, supporting the potential for carbon storage in the coming decades.

Bell-shaped thermal niche curve: Tree growth showed a non-linear increase up to a peak around 13-14 °C, indicating an optimal temperature for tree growth in cold climates. This turning point suggests that even species found within relatively small geographical ranges can adapt and thrive in response to climate variations.

# The Case of Meltwater Runoff

## Objective

In this chapter, we will handle data of glacier using QGIS with the aim of calculating the total volume of water resulting from glacier melt that will flow into delineated catchments and will compare melting rate from the past and the future projections, using climate data downloaded form ERA5 for the past years and CORDEX for the future. The SAGA tools on QGIS will be utilized for the regions of Valle d'Aosta and Piedmont. The specific goals are to:

1. Delineate catchments in Valle d'Aosta and Piedmont with SAGA tools in QGIS;
2. Calculate the volume of water from glacier melt within these catchments.
3. Explore how different climate scenarios (RCPs) might impact glacier melt and runoff in the future projections and compared to past rate of melting water;

This work aims to provide valuable insights into the hydrological implications of glacier melt in these regions, which are critical for water resource management, ecological sustainability, and regional planning.

## Materials and methods

### Glacier Data

The glacier data used in this study were extracted from the Global Land Ice Measurements from Space (GLIMS) portal. GLIMS is an initiative designed to monitor the world's glaciers primarily using data from optical satellite instruments [a]. GLIMS provides comprehensive data on glaciers worldwide, including different attributes. This dataset is crucial for understanding the spatial distribution and physical characteristics of glaciers in Valle d'Aosta and Piedmont. The table below summarizes the attributes of the glacier data used in this works, extracts from [b]:

| FIELD NAME | DESCRIPTION |
|---|---|
| LINE_TYPE | Category of line segment. Possible values include: "glac_bound" (glacier boundary), "intrnl_rock" (internal rock outcrop, or nunatak), "snowline", "centerline" (center flowline of the glacier). |

| | |
|---|---|
| GLAC_ID | The GLIMS glacier ID |
| ANLYS_TIME | Representative time the analysis was carried out. |
| AREA | Map-plane area of the glacier, as provided by the analyst, $km^2$. |
| DB_AREA | Map-plane area of the glacier, as calculated within the GLIMS Glacier Database, $km^2$. |
| WIDTH | Representative width of the glacier, meters. |
| MIN_ELEV | Elevation of the lowest part of the glacier, in meters above sea level. |
| MAX_ELEV | Elevation of the highest part of the glacier, in meters above sea level. |
| SRC_DATE | The as-of date for the outline. Usually the acquisition date of the image. |

*Table 1: Attributes of the glacier from GLIMS [a]*

This data allows for precise identification and measurement of glaciers, facilitating accurate calculations of meltwater volumes.

Not all the data downloaded from the GLIMS website were reliable and up-to-date. For the analysis of the glacier area, the latest update dates back to 2022, with some glacier units updated to 2021. Among the 2022 data for the area, only those with the most recent image acquisition date (SRC_DATE) were considered. For the thickness, since we were unable to find recent up-to-date data that were accurate for the entire glacier surface, we assumed an average thickness of 30 m and 100 m for all glaciers, to cover a significant range for the purpose.

## Catchments in Valle d'Aosta and Piedmont with SAGA tools in QGIS

Valle d'Aosta and Piedmont

The hydrographic network for Valle d'Aosta and Piedmont was created using SAGA tools on QGIS. We utilized the Digital Elevation Model (DEM) downloaded from the Shuttle Radar Topography Mission (SRTM) portal. SRTM DEMs provide high-resolution topographic data, which is essential for accurate hydrological modeling. SAGA's tools facilitated the delineation of river networks and catchment areas based on the DEM. The steps involved in creating the hydrographic network included:

→ **DEM Processing**: The DEM was processed to remove any sinks and ensure accurate flow direction with SAGA tools.
→ **Flow Accumulation**: Flow accumulation maps were generated to identify potential river courses.
→ **Catchment Delineation**: Catchment areas were delineated based on the flow direction and accumulation data. The catchment were delineated using the 'Upslope Area' function in SAGA, following the course of the Dora Baltea river, with the method Deterministic 8 (D8) (*This is the classical method in which water flow moves from the center of one cell to the center of one of the cells surrounding the first cell. This restricts the flow direction to multiples of 45 using 8 flow directions) [c].* The delineation was performed for specific points: Courmayeur, Lasalle, Gressan, Nus, St. Vincent, Donnas, Tavagnasco and Vilareggia.

Here a table with the coordinates of each catchment:

| Catchment name | X | Y | Location |
|---|---|---|---|
| Courmayer_catch | 342045,36 | 5072117,31 | Courmayer |
| LaSalle_catch | 349190,71 | 5067379 | La Salle |
| Gressan_catch | 366895,23 | 5065286,16 | Gressan |
| Nus_catch | 383280,06 | 5063957,158 | Nus |
| StVincent_catch | 394294,29 | 5066449,993 | St. Vincent |
| Donnas_catch | 404351,77 | 5050251,609 | Donnas |
| Tavagnasco_catch | 408138.8 | 5044987.4 | Tavagnasco |
| Villareggia_catch | 417526.4 | 5017993.8 | Villareggia |

*Table 2: Coordinates of delineated catchments*

Before conducting the analysis, all datasets were integrated into a unified spatial reference system (WGS 84 / UTM zone 32N). This ensured consistency and accuracy in spatial analyses. Additionally, the data were preprocessed to remove any inconsistencies or errors, such as overlapping polygons or incorrect attribute values.

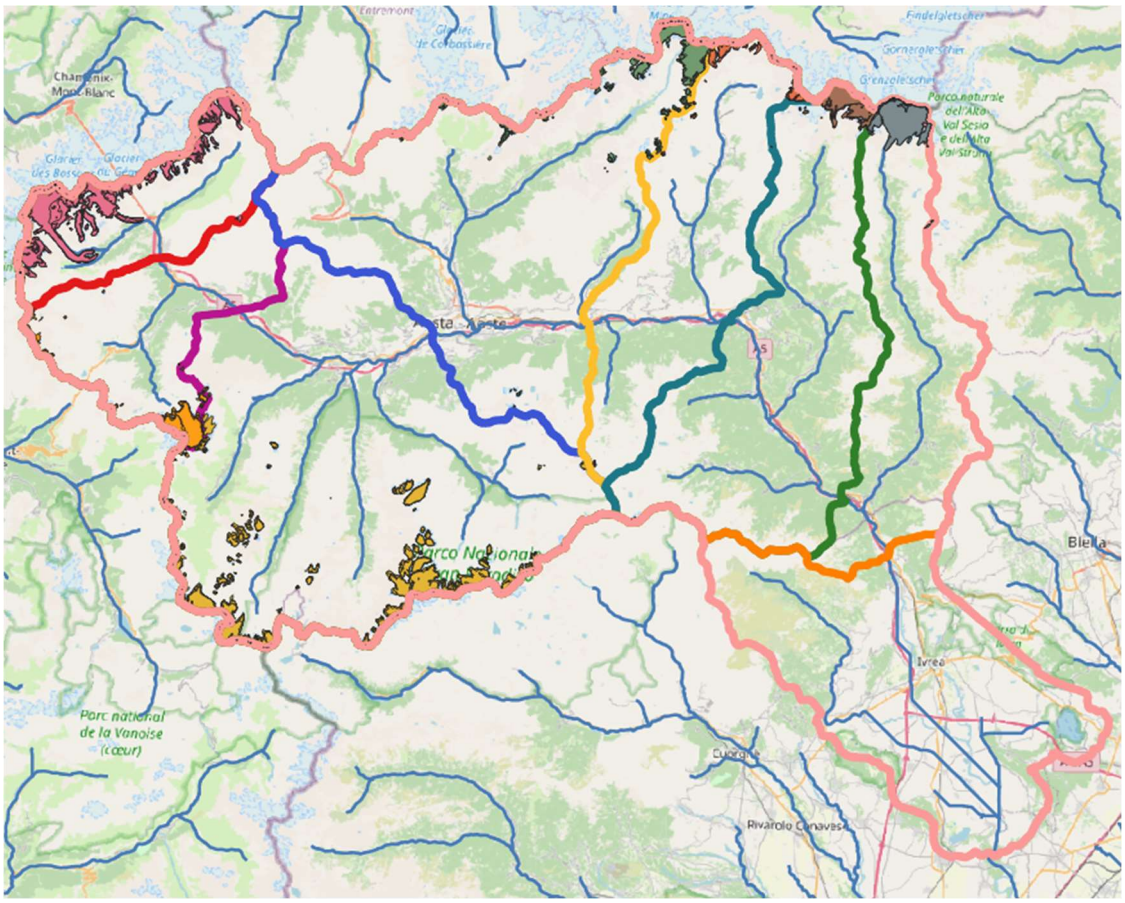

Figure 5: Catchment area and glacier polygons in the area of Valle D'Aosta and Piedmont trough Dora Baltea river from Qgis

## Volume of water from glacier melt within these catchments

To calculate the volumes of meltwater, after the delineation of the catchments, a few steps were done:

1. **Glacier Polygons Selection**: Polygons of glaciers within each catchment area were selected. This was done using spatial queries in QGIS to identify glaciers intersecting the catchment boundaries.
2. **Attribute Extraction**: The attribute table for these selected glacier polygons was exported to Excel. This table included information on glacier line type, area, data of acquisition image and other relevant attributes.
3. **Volume Calculation**: The volume of meltwater was calculated by multiplying the area of each glacier polygon, extracted using the field calculator in QGIS ($area) by an assumed average thickness of 30 m and 100 m. This simplified approach provides a first-order estimate of the meltwater volume, which can be refined with more detailed data and modeling. The calculated volume of the glaciers was converted into water equivalent volume, switching from the density of ice to density of water. For each catchment, it was summed while descending along the Dora Baltea, reaching the Villareggia catchment, which contains the total glacier volume. Below is a representative histogram.

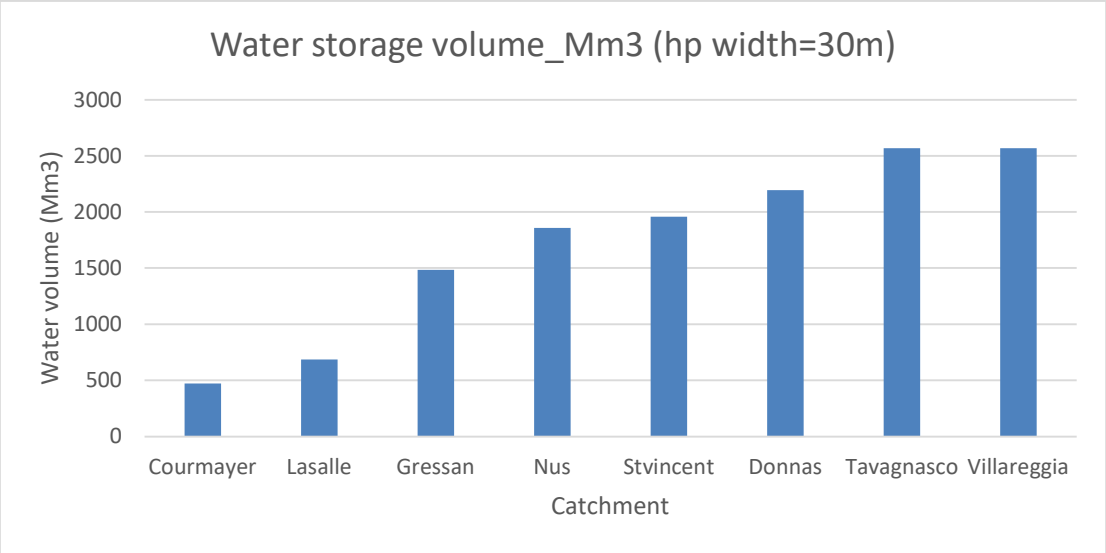


*Figure 6: Water storage volume Mm3 (hp width = 30m)*

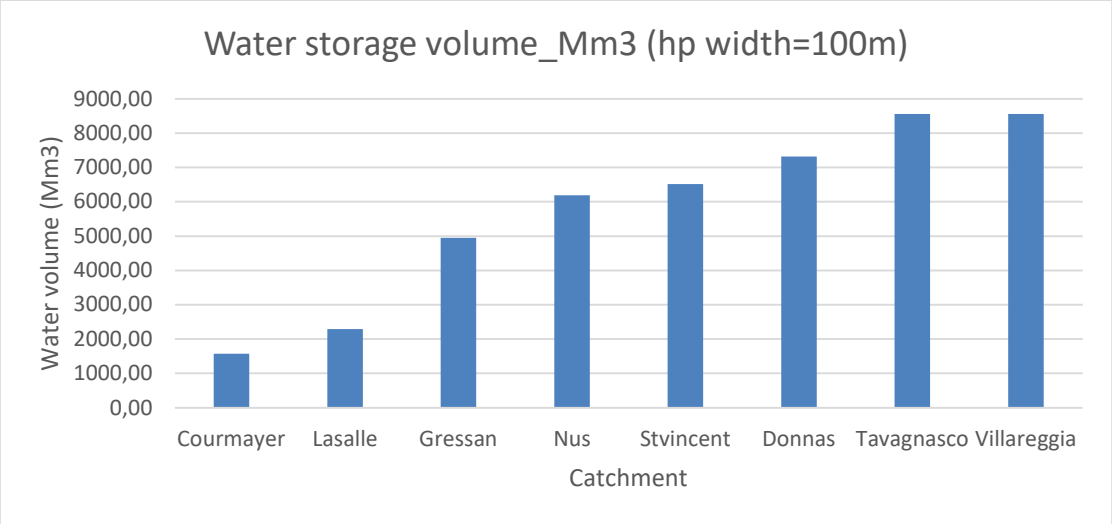


*Figure 7: Water storage volume Mm3 (hp width = 100m)*

This total glacier volume was compared to the volume of the hydrographic basins in Piedmont and Aosta Valley, and the total volume, when the hypothesed width is 30m, is approximately equal to about 10 times the volume of Lake Garda and, when the hypothesed width is 100m, is approximately equal to about 19 times the volume of Lake Garda. [d]

## How different climate scenarios (RCPs) might impact glacier melt and runoff in the future projections and compared to past rate of melting water

Materials and methods

*Past years*

For the comparison with previous years, we downloaded the hourly temperature data for the years 2020, 2021, and 2022 from the ERA5 portal, focusing on the area of our interest.

ERA5 offers hourly estimates for a wide array of atmospheric, ocean-wave, and land-surface variables. To estimate uncertainties, a 10-member ensemble is sampled every three hours. For convenience, the ensemble mean and spread are pre-computed. These uncertainty estimates are closely linked to the evolving observing system and highlight flow-dependent sensitive regions. Additionally, monthly-mean averages are pre-calculated for numerous climate applications, although the ensemble mean and spread are not available as monthly means.[e]

ERA5 updates daily with approximately a 5-day delay. If significant flaws are identified in this preliminary release (known as ERA5T), the data may differ from the final release issued 2 to 3 months later, with notifications provided to users in such cases.[e]

The data has been regridded to a regular latitude-longitude grid with a resolution of 0.25 degrees for reanalysis and 0.5 degrees for uncertainty estimates (0.5 and 1 degree respectively for ocean waves). There are four main subsets: hourly and monthly products, available both on pressure levels (upper air fields) and single levels (atmospheric, ocean-wave, and land surface quantities).[e]

*Future years*
To handle the future forecast data, they were downloaded from CORDEX, for various climate scenarios including the best-case RCP2.6 and the worst-case RCP8.5, analyzed through different climate models. In this research, two models were used: CNRM-CM5 and MPI-ESM-LR.

*CORDEX*
It offers Regional Climate Model (RCM) data on single levels from various experiments, models, domains, resolutions, ensemble members, time frequencies, and periods, calculated over multiple regional domains globally within the framework of the Coordinated Regional Climate Downscaling Experiment (CORDEX). The term "single levels" indicates that the variables are 2D matrices computed at a specific vertical level, which may be at the surface or a particular pressure level in the atmosphere. This entry does not include multiple vertical levels.[i]

High-resolution Regional Climate Models (RCMs) provide detailed climate change information on regional and local scales that coarse-scale Global Climate Models (GCMs) cannot offer. This results in better descriptions of small-scale regional climate characteristics and more accurate representations of extreme events. As such, RCM outputs are crucial for regional and local climate impact studies and adaptation planning. RCMs rely on GCMs for lateral and lower boundary conditions, effectively acting as magnifying glasses for GCMs.[i]

CORDEX experiments comprise RCM simulations for various future socio-economic scenarios (forcings), different combinations of GCMs and RCMs, and

multiple ensemble members of the same GCM-RCM combinations. This experimental design allows for addressing key uncertainties in future climate change due to different socio-economic development scenarios, imperfections in regional and global models, and natural climate system variability.[i]

This design facilitates investigations into several critical questions about future climate change:
*What will future climate forcing be?*
*How will the climate system respond to changes in forcing?*
*What is the uncertainty related to the natural variability of the climate system?*

The term "experiment" in the CDS form refers to three main categories:
Evaluation: CORDEX experiments driven by ECMWF ERA-Interim reanalysis for a past period (typically 1980-2010). These experiments evaluate the quality of the RCMs using perfect boundary conditions from a reanalysis system. [i]

Historical: CORDEX experiments covering periods with modern climate observations (typically 1950-2005). Boundary conditions are provided by GCMs, and these experiments follow observed climate forcing changes, serving as a reference period for future scenario comparisons. [i]

Scenario: CORDEX climate projection experiments using RCP (Representative Concentration Pathways) scenarios (RCP 2.6, 4.5, and 8.5) for future climate forcing. Boundary conditions are provided by GCMs, covering the period 2006-2100.[i]

The Representative Concentration Pathways (RCPs) effectively capture the range of greenhouse gas (GHG) emissions found in broader literature. These pathways include a stringent mitigation scenario (RCP2.6), two intermediate scenarios (RCP4.5 and RCP6.0), and one scenario with very high GHG emissions (RCP8.5). Scenarios without additional efforts to constrain emissions, known as ‘baseline scenarios,’ lead to pathways ranging between RCP6.0 and RCP8.5. RCP2.6 represents a scenario aimed at keeping global warming likely below 2°C above pre-industrial levels. Most models suggest that achieving forcing levels similar to RCP2.6 requires substantial net negative emissions by 2100, averaging around 2 GtCO2 per year. The land use scenarios in the RCPs show a wide range of possible futures, from net reforestation to further deforestation, aligning with projections in the broader scenario literature. For air pollutants such as sulfur dioxide (SO2), the RCP scenarios assume a consistent decrease in emissions due to assumed air pollution control and GHG mitigation policies. Importantly, these future scenarios do not account for potential changes in natural forcings. [15]

RCP2.6 and RCP8.5 represent the extremes of greenhouse gas emissions scenarios in current literature. RCP2.6 illustrates a future with low GHG emissions and significant mitigation efforts, providing about a 67% chance of keeping global

warming below 2ºC by 2100, according to CMIP5 simulations. On the other hand, RCP8.5 describes a future with high GHG emissions where no climate policies are implemented, resulting in continuous and substantial increases in atmospheric GHG concentrations. Among all the RCPs, RCP8.5 represents the scenario with the highest emissions. [16]

| | Near-term: 2031–2050 | | End-of-century: 2081–2100 | |
|---|---|---|---|---|
| Scenario | Mean (°C) | *Likely* range (°C) | Mean (°C) | *Likely* range (°C) |
| RCP2.6 | 1.6 | 1.1 to 2.0 | 1.6 | 0.9 to 2.4 |
| RCP4.5 | 1.7 | 1.3 to 2.2 | 2.5 | 1.7 to 3.3 |
| RCP6.0 | 1.6 | 1.2 to 2.0 | 2.9 | 2.0 to 3.8 |
| RCP8.5 | 2.0 | 1.5 to 2.4 | 4.3 | 3.2 to 5.4 |

*Table 3: Projected global mean surface temperature change relative to 1850–1900 for two time periods under four RCPs*

Climate models are simulators of the climate itself and generate climate data. The generated data is gridded data which means they are available on a grid all over the world. Climate models give in output data on a numerical grid with finite points. For each grid point the model gives you the measured variables. The data is saved with correct data formats. [17]

We use climate models in order to do future projections. Many groups in the world are using their models to do future projections: the problem is that if everybody does it slightly differently, results are not easily comparable, this is the reason why many years ago a series of coordinated international model intercomparison projects where set up.
CMIP: the reason of the name is because the models which are being compared are mainly coupled models (a coupled climate model is a computer code that estimates the solution to differential equations of fluid motion and thermodynamics to obtain time and space dependent values for temperature, winds and currents, moisture and/or salinity and pressure in the atmosphere and ocean).
CMIP5 is the most recent and was done around 2011.

It's a big effort to bring together all the modeling groups in the world, everyone who is developing a climate model is asked to perform common experiments in which everyone follow certain rules and steps:

- They're asked to reconstruct the climate from 1850 to today;
- Then, they're asked to do experiments like the increase in CO2 every year by 1%;
- Finally, they have to produce future scenarios.

By doing all these ecperiments, we have a series of model experiments which differ only by the model which has perform the integration; these models are very different from each other because they may contain different physical parametrization. [17]

*CNRM-CERFACS CNRM-CM5*

The CNRM-CERFACS CNRM-CM5 climate model is a comprehensive tool developed by the Centre National de Recherches Météorologiques (CNRM) and the Centre Européen de Recherche et Formation Avancée en Calcul Scientifique (CERFACS). It is used to study climate variability and change over various timescales, from months to centuries.

The CNRM-CM5 integrates several sub-models:
Atmosphere: ARPEGE-Climat v5.2, operating with a spectral resolution of T127 (~1.4° x 1.4°) and 31 vertical levels. This model includes variables such as temperature, specific humidity, and ozone concentration. [a] [f]
Ocean: NEMO v3.2, developed by the NEMO consortium, with a horizontal resolution of ~1° and 42 vertical levels. [f]
Sea Ice: GELATO v5, models sea ice processes and their interactions with the ocean and atmosphere. [f]
Land Surface: SURFEX, using the ISBA scheme for modeling land processes and surface-atmosphere fluxes. [f]
Rivers: TRIP (Total Runoff Integrating Pathways) for simulating river routing and water discharge.[f]

The CNRM-CM5 model is used for:
Historical Climate Reconstructions: Simulating climate from 1850 to present.
Future Climate Projections: Based on various greenhouse gas scenarios.
Paleo-climate Studies: Including the last interglacial and last glacial maximum periods.
Seasonal Forecasts: For short-term climate predictions. [f] [g]

Resolution: Improved horizontal resolution in atmospheric and oceanic components compared to previous versions.
Radiative Transfer: Incorporates the Rapid Radiation Transfer Model (RRTM) for longwave radiation and an upgraded shortwave radiation scheme.[13]
Aerosols: Enhanced parameterization of direct and indirect aerosol effects.
Convection: Deep convection scheme for simulating cloud processes and vertical moisture transport.[13]

*MPI-M-MPI-ESM-LR*

The MPI-M-MPI-ESM-LR (Max Planck Institute for Meteorology Earth System Model, Low Resolution) is a comprehensive climate model developed by the Max Planck Institute for Meteorology. It is designed to simulate the Earth's climate system, including interactions between the atmosphere, ocean, and land surfaces. This model is part of the Coupled Model Intercomparison Project Phase 5 (CMIP5), which aims to improve our understanding of past, present, and future climate changes.

The MPI-ESM-LR integrates several key components:

Atmosphere: The atmospheric component uses ECHAM6 with a horizontal resolution of T63 (approximately 1.875° x 1.875°) and 47 vertical levels. This component includes various physical processes such as radiation, convection, and cloud formation. [14]
Ocean: The ocean component, MPIOM, operates with a nominal resolution of 1.5° and 40 vertical levels. It simulates ocean currents, temperature, salinity, and sea ice dynamics. [14]
Land Surface: The JSBACH land surface model includes processes such as soil hydrology, vegetation dynamics, and carbon cycling [14]

The MPI-ESM-LR is used for a wide range of climate simulations, including:
Historical Simulations: Reconstructing climate conditions from 1850 to the present to understand long-term trends and variability.
Future Projections: Predicting climate changes under various greenhouse gas emission scenarios up to the year 2100.
Paleo-climate Studies: Investigating past climates such as the last glacial maximum and the Holocene epoch. [14] [h]

Resolution: The MPI-ESM-LR features enhanced resolution in both the atmosphere and ocean components, improving the representation of small-scale processes and interactions.
Carbon Cycle: It incorporates detailed representations of the global carbon cycle, including terrestrial and oceanic carbon sinks and sources. [14]
Interactive Aerosols: The model includes interactive aerosols, which are crucial for accurately simulating radiation balance and cloud formation processes.[14]

## Methods

All data manipulation for the glaciers was performed using MATLAB software.
Let's start with the historic data 2020, 2021, 2022.
*Combine 3 separate NetCDF files (2020, 2021, 2022)*
For the past years it was combined the three separate NetCDF files containing historical data (2020, 2021, and 2022) into a single NetCDF file. The script reads the surface temperature variable (t2m) and the time variable from each file for the years 2020, 2021, and 2022. The temperature data (t2m) and the time data are concatenated along the time dimension. It defines the dimensions of the variables (latitude, longitude, and time) for the combined file. A new NetCDF file called 'combined_historic.nc' is created, it writes the coordinate data and the concatenated t2m and time data into the new NetCDF file.

*Aggregate NetCDF*
The script processes temperature data for eight glaciers by aggregating historical temperature data from NetCDF files. It combines hourly data into monthly and

annual averages and saves the results in CSV files for each glacier. Glacier bounding box information is read from an Excel file called glacier_boundaries.xlsx.

The script loops through each glacier, extracting its name and bounding box coordinates. It rounds the bounding box coordinates to match the resolution of the temperature data and extracts the latitude and longitude indices that fall within the glacier's bounding box. It reads temperature data for the specified bounding box and time period from the NetCDF file, then aggregates the hourly temperature data spatially by averaging along the longitude and latitude dimensions. The hourly data is then aggregated temporally to compute monthly and annual means using a function called aggregate_historic_T_data.

The script creates CSV filenames using the glacier names and saves the monthly and annual mean temperature data as CSV files for each glacier, making it easier to analyze and utilize the temperature data in further research or applications. Functions used in the script include get_ncfile_bbox, which rounds the bounding box coordinates to match the grid of the NetCDF data, and aggregate_historic_T_data, which converts hourly temperature data into monthly and annual averages. These functions take inputs such as shapefile bounding box, historic flag, time values, and hourly temperature data, and output the rounded bounding box and timetables of monthly and annual mean temperatures, respectively.

*Extraction of zcell and correction of temperature of the glacier*
Temperature is strongly dependent on elevation. A simple linear regression reads

$$\mathrm{T(z)} = \mathrm{T_0} - \mathrm{b} \cdot \mathrm{z}$$

with the slope b called "lapse rate" [in °C/1000m]
Typical values of b are **5 - 6 °C/1000m** but local values can be obtained using measured T at different elevations and interpolating with a linear regression. [18]

Having the temperature in a big cell (containing the glacier) $T_{cell}$ and knowing the mean elevation of the cell, $z_{cell}$, and that of the glacier, $z_{glacier}$, we can write:

$$T_{glacier} = T_{cell} - b \cdot (z_{glacier} - z_{cell})$$

[18]

The z of the cell of the NetCDF has been extrapolated using the variable geopotential. With the script we begins by initializing necessary variables and constants, including the gravitational acceleration.
Next, it reads latitude and longitude data from a NetCDF file containing geopotential data.

The script then reads boundary information for each glacier from an Excel file.
For each glacier, it extracts the bounding box (bbox) and adjusts it to match the grid resolution of temperature data from another NetCDF file.

Using this adjusted bbox, it filters and retrieves elevation data from the geopotential NetCDF file, converting it from geopotential height to actual elevation.
The elevation data is aggregated spatially and temporally by computing the mean values across longitude, latitude, and time dimensions.
These mean elevation values are stored in a new column in the original Excel file containing glacier data.
Finally, the updated table, now including the historic elevation data, is saved to a new Excel file.

This process ensures that each glacier's elevation data is accurately processed and integrated into the existing dataset for further analysis or reporting purposes.

*Monthly Melting Rate (MR) for each glacier*

Melting, $M$, expressed as liquid water depth per unit time, depends on temperature, as a proxy of energy (or heat) availability.
The formula is

$$M = D_f \cdot (T_i - T_0)$$

where $M$ is meltwater depth [in mm/day]
$(T_i - T_0)$ is the air temperature departure from reference (degree day) in given day
$D_f$ is the "degree-day factor" [mm/°C /day] conversion factors, that differentiates between melting of snow and ice. For the degree day factor we use the value of 5.5 mm/°C /day, deriving it from literature for the melting of the ice. [18] [19]

The script retrieves elevation data for historic periods (2020-2022) of 8 glaciers using MATLAB.
This script performs temperature correction and calculates melting rates for each glacier based on monthly temperature data contained in CSV files. Here's a summary of what the script does:
It starts by defining constants and reading glacier information from an Excel file (glacier_boundaries_with_all_elevations.xlsx).
Next, it sets the folder path (folder_path) containing CSV files with temperature data. This path can be adjusted to select different climate scenarios (e.g., historical data or future projections).
It defines a subfolder (output_folder_path) named 'MR' within folder_path to save processed files.
Each CSV file is then processed as follows:

- → Reads the CSV file into a table.
- → Checks for the existence of the "monthly_means" column; if not, it reads the "annual_means" or "Temperature" column.
- → Creates a new column "Tcell_C" by converting temperatures from Kelvin to Celsius, if necessary.
- → Calculates the new "Tglacier_C" column, which represents corrected glacier

temperatures based on elevation.

→ Computes the new "MR" column, representing the melting rate based on corrected glacier temperatures.

→ Replaces all negative values in the "MR" column with 0.

→ Saves the updated table to a CSV file with the appropriate name in the 'MR' subfolder.

Finally, the script prints a message for each processed file, indicating the name of the output file.

*Weight average of Melting Rate (MR)*

This script processes multiple CSV files containing monthly mean melting rate (MR) data for different glaciers.

Inputs:

→ Glacier Information Excel File (glacier_boundaries_with_all_elevations.xlsx):

→ Contains information about glaciers, including names and area (used as weights).

→ Folder Path:

→ Specifies the directory (historic in this case) where the CSV files with MR data are located.

→ This path can be adjusted to other scenarios (future_T_rcp26_CNRM_CM5, future_T_rcp85_CNRM_CM5, etc.).

Processing Steps:

→ Read Glacier Information:Reads the glacier information from the Excel file into a table (glacier_info).

→ Set Folder Paths: Constructs paths to the folder (MR subfolder within historic) where processed data will be stored.

→ Initialize Storage Structures: Prepares to store MR columns from each CSV file in a cell array (MR_columns).

→ Loop Through Each CSV File: Iterates through each CSV file in the specified folder (MR files ending with monthly_mean_timetable_MR.csv). Reads each CSV file into a table (data). Extracts the date or time column (monthly_mean_dates or Time) from the first file and stores it in combined_data. Extract and Store MR Data

→ Calculate Weighted Average MR: Computes the weighted average of MR across all files. Retrieves the glacier area (weight) from glacier_info based on the glacier name extracted from each filename. Accumulates the weighted MR values based on glacier area.

→ Normalize Weighted MR: Normalizes the accumulated weighted MR values by dividing by the sum of weights (sum(weights)).
→ Save Combined Data: Adds the normalized weighted MR column (MR_weighted) to combined_data. Writes combined_data to a new CSV file (combined_MR_weighted.csv) in the MR subfolder.

Outputs:
Combined Data CSV File (combined_MR_weighted.csv): Contains the original date or time column (Date) and dynamically named MR columns (MR1, MR2, ...) from each CSV file. Includes a final column (MR_weighted) representing the normalized weighted average melting rate across all glaciers.

This script effectively processes multiple MR data files, computes weighted averages, and consolidates results into a single CSV file for further analysis or reporting.

Results and comparison

The script has successfully computed and weighted the melting rates for each glacier based on its surface area. Subsequently, it calculated the weighted average melting rate across glaciers. This approach ensures that larger glaciers, with greater surface areas, contribute proportionally more to the averaged melting rate.

To effectively visualize and compare the results with previous years, the weighted monthly melting rates for the years 2020, 2021, and 2022 have been plotted. As anticipated from historical temperature trends, 2022 exhibits the highest melting rate compared to the other years.

This analysis underscores the script's capability to integrate spatial glacier characteristics, such as area, into the calculation of melting rates. Moreover, the plotted data provides a clear depiction of the variations in melting rates over the specified time frame, emphasizing the heightened melting observed in 2022 relative to preceding years.

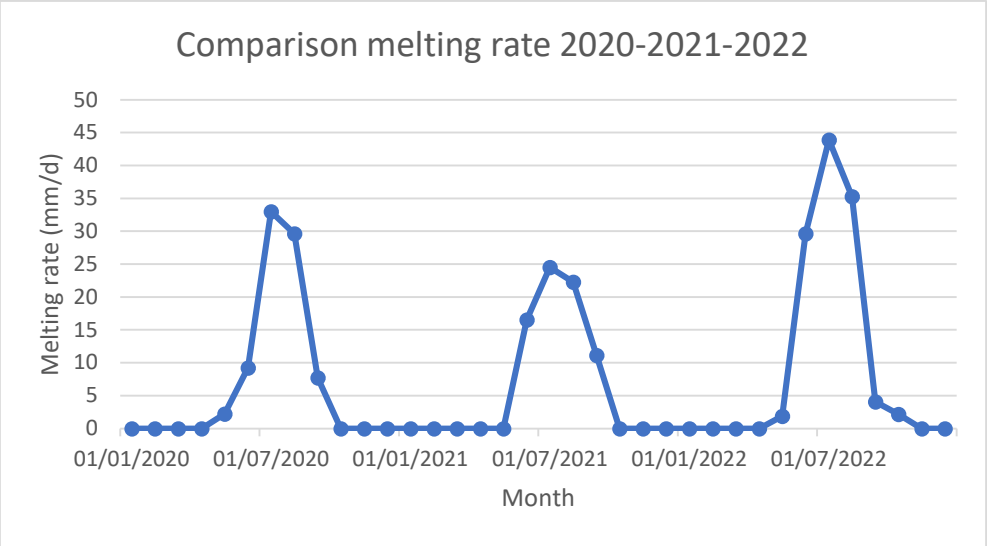


*Figure 8: Historical melting rate (mm/d) 2020-2021-2022*

For the calculation of the total volume of ice melted each year, we use the formula:

$$Vtot = MR \cdot Areatot \cdot 365$$

Where:

- → MR is the mean weighted melting rate from the 12 month in every year (m/d)
- → Areatot is the sum of the are of all the glaciers taking into consideration ($m^2$)
- → 365 are the day in a year to switch from days to year

The computed volumes for each year (2020, 2021, and 2022) were compared to assess yearly variations in ice melt. This comparative analysis provides insights into the annual dynamics of glacier melting, highlighting any significant differences or trends observed across the specified years.

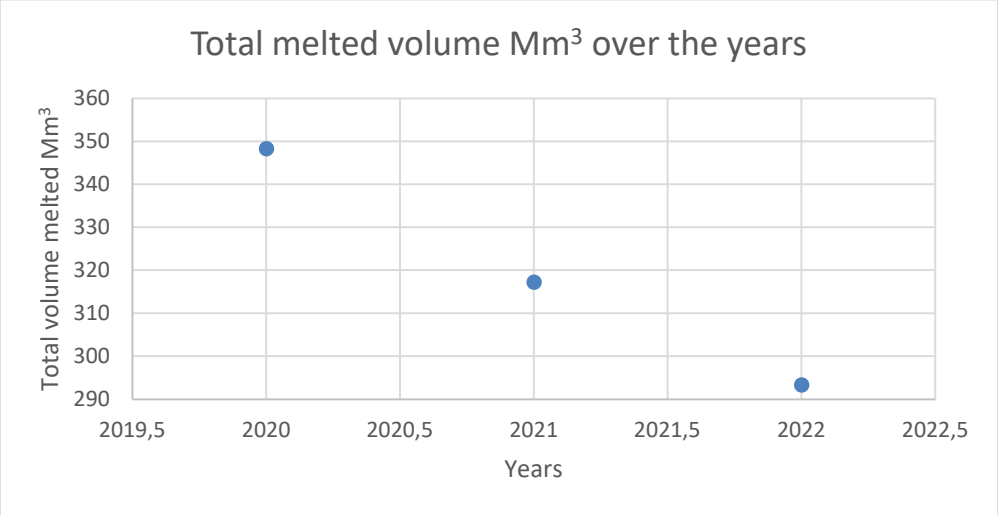


*Figure 9: Total melted volume over 2020-2021-2022*

| Year | Total volume melted Mm3 |
|---|---|
| 2020 | 348,31 |
| 2021 | 317,27 |
| 2022 | 293,36 |

*Table 4: Total melted volume over 2020-2021-2022*

The lower value in 2022 is due to the lower value of area total of the gacier

*Future projections*

All data manipulation for the glaciers was performed using MATLAB software.
Let's look at the future projections.

*Aggregate NetCDF*

The script provided performs aggregation and saving of temperature data from NetCDF files for future climate projections (2051-2060) for each of the 8 glaciers. Here's a detailed explanation:
The script iterates through each glacier, extracting its bounding box (bbox) coordinates. It filters temperature data (tas) based on the bbox coordinates to include only relevant grid cells. It creates a logical mask (lonlatCheck) to identify spatially-overlapping grid cells within the bbox.
Temperature data (tas) is extracted using logical indexing to select grid cells identified by lonlatCheck.
The selected data is reshaped to handle the time dimension properly and compute monthly mean temperatures (glacier_tas_monthly).
The script calls a function (aggregate_future_T_data) to aggregate hourly temperature data into monthly and annual means (monthly_mean_tt and annual_mean_tt).
For each glacier, two CSV files are generated: one containing monthly mean temperatures (*_monthly_mean_timetable.csv) and another containing annual mean temperatures (*_annual_mean_timetable.csv).

The script efficiently processes temperature data for multiple glaciers, aggregates spatially and temporally, and saves the results in CSV format. This approach facilitates further analysis and comparison of climate projections across different glaciers and scenarios.

*Extraction of zcell and correction of temperature of the glacier*

Temperature is strongly dependent on elevation. A simple linear regression reads

$$T(z) = T_0 - b \cdot z$$

with the slope b called "lapse rate" [in °C/1000m]
Typical values of b are **5 - 6 °C/1000m** but local values can be obtained using measured T at different elevations and interpolating with a linear regression. (Libro professoressa)
Having the temperature in a big cell (containing the glacier) $T_{cell}$ and knowing the mean elevation of the cell, $z_{cell}$, and that of the glacier, $z_{glacier}$, we can write:

$$T_{glacier} = T_{cell} - b \cdot (z_{glacier} - z_{cell})$$

(Libro professoressa)
For the fixed value of b, we used 6°C/1000m.

The script provided performs the following operations for each of the 8 glaciers:
The script initializes constants and paths to NetCDF files (elevation_data_CNRM_fn and elevation_data_MPI_fn) containing elevation data.
It reads latitude (latValuesCNRM, latValuesMPI) and longitude (lonValuesCNRM, lonValuesMPI) data from these NetCDF files.
Glacier boundaries (minLon, minLat, maxLon, maxLat) are read from an Excel file (glacier_boundaries_with_historic_elevation.xlsx).
The script initializes variables (glacierNames, minLons, minLats, maxLons, maxLats) to store these boundaries.
The script iterates through each glacier, extracting its bounding box (glacier_bbox).
It filters elevation data (elevationCNRM and elevationMPI) based on the bounding box coordinates to include only relevant grid cells (lonlatCheckCNRM and lonlatCheckMPI).
Elevation data is extracted using logical indexing to select grid cells identified by lonlatCheckCNRM and lonlatCheckMPI.
The selected data is averaged to compute the mean elevation for each glacier (elevationCNRM_selected and elevationMPI_selected).

The script updates the original Excel file (glacier_boundaries_with_historic_elevation.xlsx) by adding two new columns: ElevationFutureCNRM and ElevationFutureMPI.
These columns contain the mean elevation values derived from the respective NetCDF files (elevation_data_CNRM_fn and elevation_data_MPI_fn).

The updated table, including the new elevation columns, is saved to a new Excel file (glacier_boundaries_with_elevation.xlsx).

The script effectively processes elevation data for multiple glaciers, filters based on specified geographical boundaries, computes mean elevations, and updates an Excel file for further analysis or visualization of future climate projections.

*Monthly Melting Rate (MR) for each glacier*

Melting, M, expressed as liquid water depth per unit time, depends on temperature, as a proxy of energy (or heat) availability.
The formula is

$$M = D_f \cdot (T_i - T_0)$$

where M is meltwater depth [in mm/day]
$(T_i - T_0)$ is the air temperature departure from reference (degree day) in given day
$D_f$ is the "degree-day factor" [mm/°C /day] conversion factors, that differentiates

between melting of snow and ice. As $T_0$ we hypothise 0°C, for the degree day factor we use the value of 5.5 mm/°C /day, deriving it from literature for the melting of the ice. (Libro professoressa) (Positive degree-day sums in the Alps: a direct link between glacier melt and international climate policy, Braithwhite et al. 2022)

The script retrieves elevation data for future projections (2051-2060) of 8 glaciers using MATLAB.
This script performs temperature correction and calculates melting rates for each glacier based on monthly temperature data contained in CSV files. Here's a summary of what the script does:
It starts by defining constants and reading glacier information from an Excel file (glacier_boundaries_with_all_elevations.xlsx).
Next, it sets the folder path (folder_path) containing CSV files with temperature data.
It defines a subfolder (output_folder_path) named 'MR' within folder_path to save processed files.
Each CSV file is then processed as follows:

- → Reads the CSV file into a table.
- → Checks for the existence of the "monthly_means" column; if not, it reads the "annual_means" or "Temperature" column.
- → Creates a new column "Tcell_C" by converting temperatures from Kelvin to Celsius, if necessary.
- → Calculates the new "Tglacier_C" column, which represents corrected glacier temperatures based on elevation.
- → Computes the new "MR" column, representing the melting rate based on corrected glacier temperatures.
- → Replaces all negative values in the "MR" column with 0.
- → Saves the updated table to a CSV file with the appropriate name in the 'MR' subfolder.

Finally, the script prints a message for each processed file, indicating the name of the output file.

*Weight average of Melting Rate (MR)*

This script processes multiple CSV files containing monthly mean melting rate (MR) data for different glaciers.

Inputs:

- → Glacier Information Excel File (glacier_boundaries_with_all_elevations.xlsx): Contains information about glaciers, including names and area (used as weights).
- → Folder Path: Specifies the directory where the CSV files with MR data are located. This path can be adjusted to other scenarios

(future_T_rcp26_CNRM_CM5, future_T_rcp85_CNRM_CM5, etc.).

Processing Steps:

- → Read Glacier Information:Reads the glacier information from the Excel file into a table (glacier_info).
- → Set Folder Paths: Constructs paths to the folder (MR subfolder within historic) where processed data will be stored.
- → Initialize Storage Structures: Prepares to store MR columns from each CSV file in a cell array (MR_columns).
- → Loop Through Each CSV File: Iterates through each CSV file in the specified folder (MR files ending with monthly_mean_timetable_MR.csv). Reads each CSV file into a table (data). Extracts the date or time column (monthly_mean_dates or Time) from the first file and stores it in combined_data. Extract and Store MR Data
- → Calculate Weighted Average MR: Computes the weighted average of MR across all files. Retrieves the glacier area (weight) from glacier_info based on the glacier name extracted from each filename. Accumulates the weighted MR values based on glacier area.
- → Normalize Weighted MR: Normalizes the accumulated weighted MR values by dividing by the sum of weights (sum(weights)).
- → Save Combined Data: Adds the normalized weighted MR column (MR_weighted) to combined_data. Writes combined_data to a new CSV file (combined_MR_weighted.csv) in the MR subfolder.

Outputs:
Combined Data CSV File (combined_MR_weighted.csv): Contains the original date or time column (Date) and dynamically named MR columns (MR1, MR2, ...) from each CSV file. Includes a final column (MR_weighted) representing the normalized weighted average melting rate across all glaciers.

This script effectively processes multiple MR data files, computes weighted averages, and consolidates results into a single CSV file for further analysis or reporting.

Results and comparison

The script has successfully computed and weighted the melting rates for each glacier based on its surface area. Subsequently, it calculated the weighted average melting rate across glaciers. This approach ensures that larger glaciers, with greater surface areas, contribute proportionally more to the averaged melting rate.

To effectively visualize and compare the results with future years, the future weighted monthly melting rates for the period 2051-2060 have been plotted.

This analysis underscores the script's capability to integrate spatial glacier characteristics, such as area, into the calculation of melting rates. Moreover, the plotted data provides a clear depiction of the variations in melting rates over the specified time frame, emphasizing the heightened melting observed in 2022 relative to preceding years.

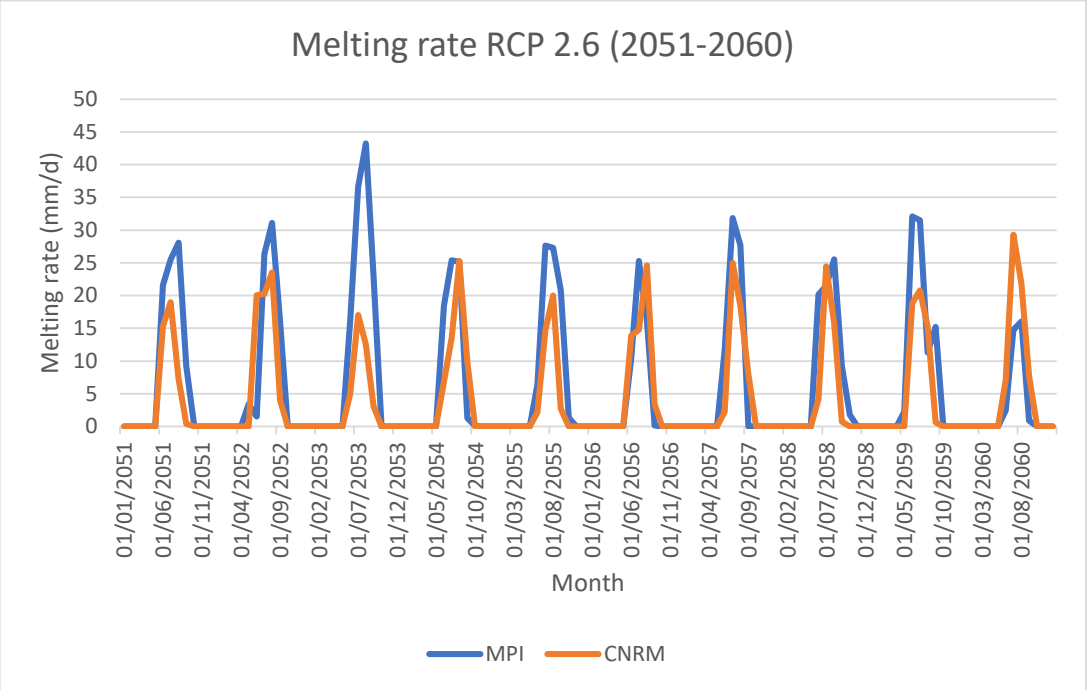


*Figure 10: Melting rate in RCP2.6 scenario with 2 different climate model*

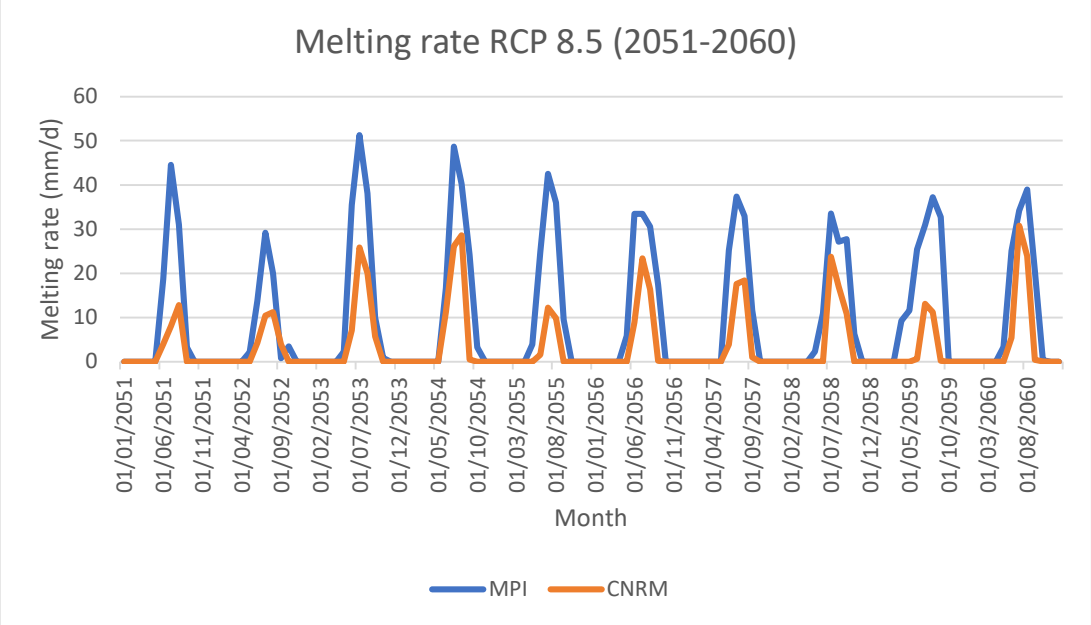


*Figure 11: Melting rate in RCP8.5 scenario with 2 different climate model*

In the context of the RCP 2.6 scenario, there are no substantial differences between the two climate models used, whereas in the RCP 8.5 scenario, the CNRM model results are much more optimistic. This is also due to the lower average

temperatures predicted by the climate model, which have a significant impact on the formula used to calculate the melting rate. As expected, the melting rate is higher in the summer months and reaches very high values, about 60mm/day in the worst-case RCP.
It seems that in the CRNM model, temperature of the future are understimated, we didn't find any correlation in the literature, this is an area that warrants further investigation with future studies.

The observed disparity in melting rate values between MPI-ESM and CNRM-CM5 is primarily due to the distinct temperature projections made by each model. The higher temperatures predicted by MPI-ESM lead to increased melting rates, while the lower temperatures from CNRM-CM5 result in lower melting rates. Understanding and visualizing these differences are crucial for assessing the potential impacts of climate change on glaciers under different climate scenarios.

## Comparison of the precipitation value bwetween historic and future projections

For this comparison we used only data available for the future from the climate model CNRM-CM5. In order to obtain another point of comparison in terms of climatic variables, to better appreciate the changes that will occur in the coming years, and to evaluate another source of water resources, we have also analyzed the precipitation variable. For future data, the "total precipitation" variable was downloaded from ERA5, which includes: "This parameter is the accumulated liquid and frozen water, comprising rain and snow, that falls to the Earth's surface. It is the sum of large-scale precipitation and convective precipitation. Large-scale precipitation is generated by the cloud scheme in the ECMWF Integrated Forecasting System (IFS). The cloud scheme represents the formation and dissipation of clouds and large-scale precipitation due to changes in atmospheric quantities (such as pressure, temperature, and moisture) predicted directly by the IFS at spatial scales of the grid box or larger. Convective precipitation is generated by the convection scheme in the IFS, which represents convection at spatial scales smaller than the grid box. This parameter does not include fog, dew, or the precipitation that evaporates in the atmosphere before it lands at the surface of the Earth. This parameter is accumulated over a particular time period which depends on the data extracted. For the reanalysis, the accumulation period is over the 1 hour ending at the validity date and time. For the ensemble members, ensemble mean, and ensemble spread, the accumulation period is over the 3 hours ending at the validity date and time. The units of this parameter are depth in meters of water equivalent. It is the depth the water would have if it were spread evenly over the grid box. Care should be taken when comparing model parameters with observations, because observations are often local to a particular point in space and time, rather than representing averages over a model grid box" [e]. For future data, the "mean precipitation flux" variable was used, which includes: "Deposition of

water to the Earth's surface in the form of rain, snow, ice, or hail. The precipitation flux is the mass of water per unit area and time. The data represents the mean over the aggregation period" [i]. Both variables were transformed into mm/d and weighted based on the area considered for data extraction

### *Weight average of precipitation*

This script processes multiple CSV files containing monthly mean precipitation data for different glaciers.

Inputs:

- → Glacier Information Excel File (glacier_boundaries_with_all_elevations.xlsx): Contains information about glaciers, including names and area (used as weights).
- → Folder Path: Specifies the directory where the CSV files with MR data are located. This path can be adjusted to other scenarios (future_P_rcp26_CNRM_CM5, future_P_rcp85_CNRM_CM5, etc.).

Processing Steps:

- → Read Glacier Information:Reads the glacier information from the Excel file into a table (glacier_info).
- → Set Folder Paths: Constructs paths to the folder (P subfolder within historic) where processed data will be stored.
- → Initialize Storage Structures: Prepares to store P columns from each CSV file in a cell array (P_columns).
- → Loop Through Each CSV File: Iterates through each CSV file in the specified folder (P files ending with monthly_mean_timetable_P.csv). Reads each CSV file into a table (data). Extracts the date or time column (monthly_mean_dates or Time) from the first file and stores it in combined_data. Extract and Store P Data
- → Calculate Weighted Average P: Computes the weighted average of P across all files. Retrieves the glacier area (weight) from glacier_info based on the glacier name extracted from each filename. Accumulates the weighted P values based on glacier area.
- → Normalize Weighted P: Normalizes the accumulated weighted P values by dividing by the sum of weights (sum(weights)).
- → Save Combined Data: Adds the normalized weighted P column (P_weighted) to combined_data. Writes combined_data to a new CSV file (combined_P_weighted.csv) in the P subfolder.

Outputs:

Combined Data CSV File (combined_P_weighted.csv): Contains the original date or time column (Date) and dynamically named P columns (P1, P2, ...) from each CSV file. Includes a final column (P_weighted) representing the normalized weighted average melting rate across all glaciers.

This script effectively processes multiple P data files, computes weighted averages, and consolidates results into a single CSV file for further analysis or reporting.

## Results and comparison

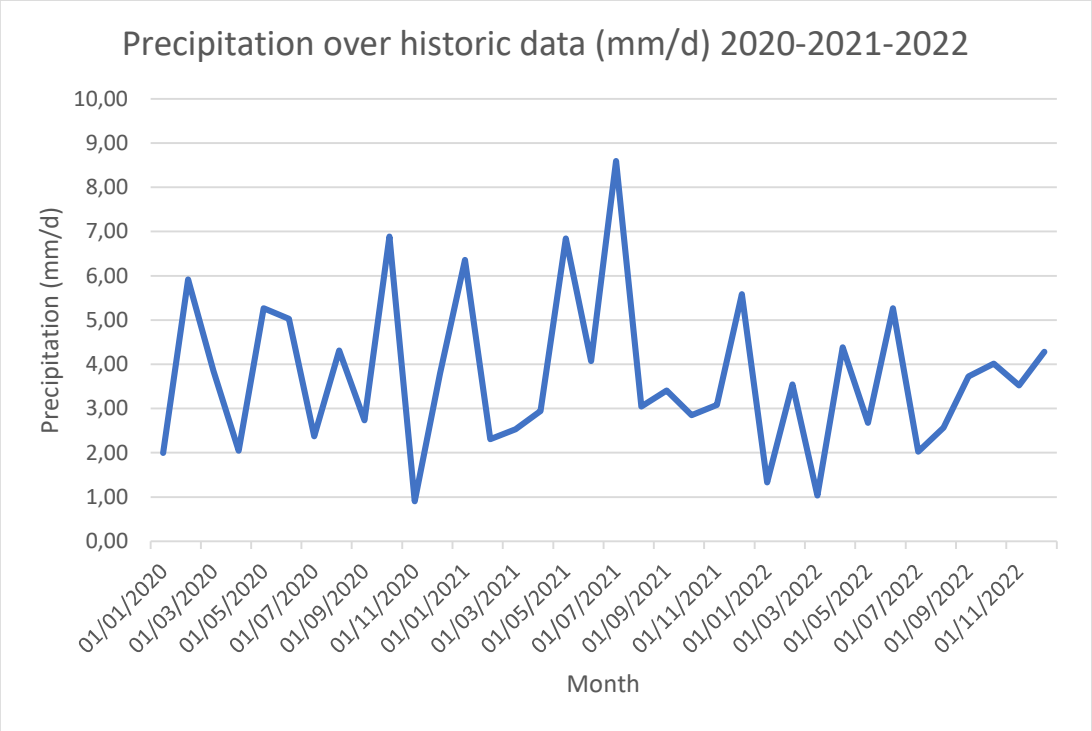


*Figure 12: Precipitation over historic data mm/d (2020,2021,2022)*

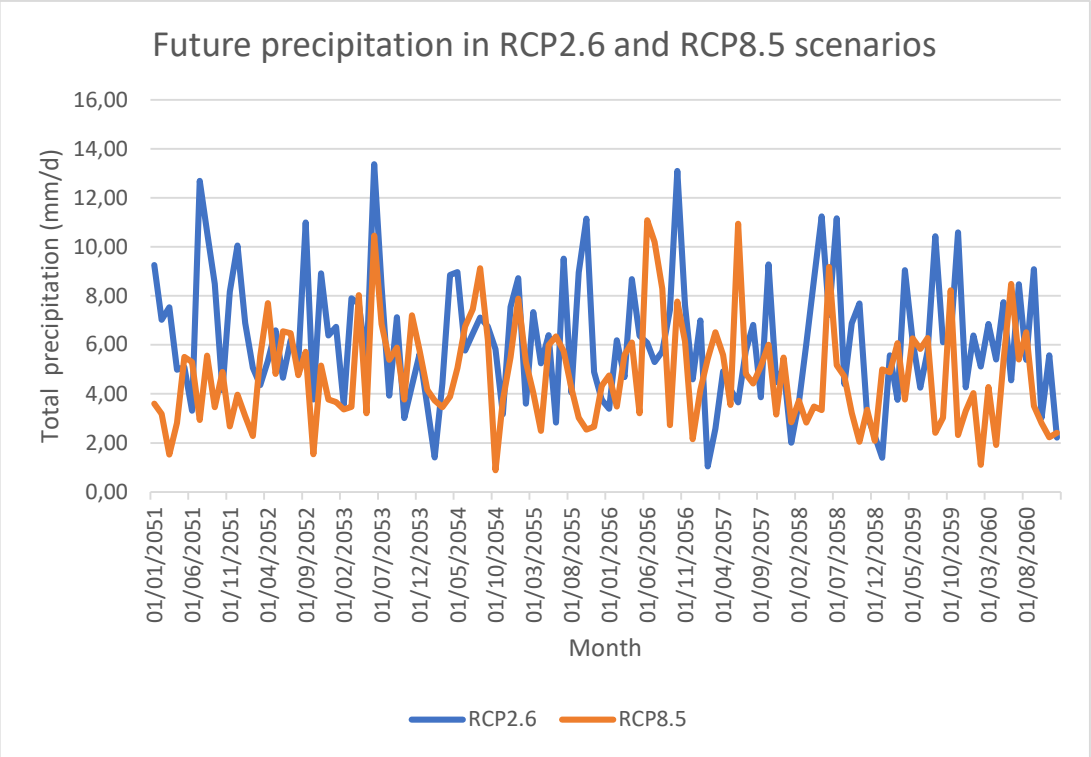


*Figure 13: Future precipitation in RCP2.6 and RCP8.5 scenarios*

Comparing the two graphs, we observed that:

**Variation and Peaks**: Historical precipitation (2020-2022) shows variability and peaks similar to those projected in the RCP 2.6 scenario, with values occasionally reaching 9 mm/d. However, in the future scenario, RCP 2.6 shows slightly higher peaks, up to 12 mm/d, suggesting an increase in precipitation variability.

**RCP 8.5 Scenario:** The RCP 8.5 scenario, with high emissions, shows a reduction in maximum precipitation peaks compared to RCP 2.6 and an increase in periods of low precipitation. This could indicate a trend towards more extreme conditions, with alternating periods of drought and intense but less frequent precipitation.

**Future Implications**: Future projections indicate that under a low emission scenario (RCP 2.6), precipitation could become more intense and variable. Conversely, under a high emission scenario (RCP 8.5), there could be a reduction in the frequency and intensity of precipitation with more prolonged periods of drought.

The analysis of historical data compared to future projections highlights a change in precipitation dynamics, with a low emission scenario predicting increased variability and intensity of precipitation, while a high emission scenario could lead to more extreme conditions with more frequent drought periods and less intense precipitation. This comparison is crucial for planning strategies to adapt to climate change, considering the impact of emissions on water resources.

## Limits of the study

The analysis of glacier surface area data encountered significant constraints due to limited data availability. Specifically, the data downloaded from the Global Land Ice Measurements from Space (GLIMS) database only included surface area measurements for the years 2021 and 2022. As a result, for the years 2020 and 2021, the surface areas for 2021 were utilized, and for 2022, the surface areas for 2022 were used. To estimate the total volume, an average of the areas from 2021 and 2022 was employed, as these areas varied only slightly, by approximately 10%.

Another limitation is that the thesis does not consider the phenomena of glacier nourishment; the glaciers are treated as static without accounting for the growth of their volume through liquid or solid precipitation. This omission means that the dynamic processes contributing to glacier mass balance, such as snowfall and rainfall, which can significantly influence glacier volume and health, are not incorporated into the analysis. Consequently, the static assumption may lead to an incomplete representation of glacier behavior over time, as it overlooks the natural cycles of accumulation and ablation that are critical to understanding glacier dynamics.

The exclusion of these factors could potentially result in an underestimation or overestimation of the glacier's future states, particularly in regions where precipitation plays a substantial role in maintaining glacier mass. This limitation underscores the complexity of accurately modeling and projecting glacier changes, as it requires comprehensive data on various climatic and environmental variables.

## Conclusions

In conclusion, the study reported data that aligns with future projections and does not present an overly pessimistic outlook. It is important to note that future data has a resolution of 0.11x0.11 (CORDEX), while past data has a resolution of 0.5x0.5 (ERA5).

The findings suggest that, despite the inherent uncertainties and limitations, the future projections are consistent with the trends observed in the historical data. The resolution differences between the CORDEX and ERA5 datasets are acknowledged, but they do not significantly undermine the overall coherence of the results.
The analysis of past and future graphs indicates that the melting rate of glaciers experienced an increase in 2022. However, future projections suggest that this rate will not see a significant increase. This provides hope that, for the next 30 years, our glacial heritage will still be partially preserved.

Regarding future projections, the melting rate as predicted by the CNRM climate in the RCP8.5 model suggests a significant decrease in the melting rate, leading to optimistic forecasts for the future climate. This projection is consistent with the average temperatures extracted from the CNRM model, which are significantly lower than those predicted by the MPI climate model. Such a reduction in the melting rate, in conjunction with lower average temperatures, paints a hopeful picture for the preservation of glacier mass in the coming decades. The favorable projections from the CNRM model offer a contrast to the more conservative estimates provided by other models, highlighting the potential for less drastic impacts of climate change on glacier dynamics. This alignment of lower temperatures and reduced melting rates strengthens the confidence in the positive outlook presented by the CNRM model.

The aspiration of this thesis is to shift the focus towards the positive aspects of climate change, aiming to harness the beneficial outcomes that may emerge in the future. Emphasizing the potential positive impacts can inspire adaptive strategies that maximize these benefits. Additionally, the thesis underscores the crucial importance of valuing and respecting water resource availability, which is essential for sustaining life on this planet.

By concentrating on positive outcomes and advocating for the prudent management of water resources, this research hopes to contribute to a more balanced and proactive approach to addressing the multifaceted challenges of climate change.

## Sitografia

[a]https://www.glims.org/
[b]https://www.glims.org/MapsAndDocs/downloaded_field_desc.html
[c]https://dges.carleton.ca/CUOSGwiki/index.php/Exploring_the_Hydrological_Tools_in_QGIS
[d]https://www.laghi.net/homepage.aspx?tab=3&subtab=2&idlago=3
[e]https://cds.climate.copernicus.eu/cdsapp#!/dataset/reanalysis-era5-single-levels?tab=overview
[f] https://www.umr-cnrm.fr/spip.php?article126&lang=en
[g] https://geomodeling.njnu.edu.cn/modelItem/4782528d-2eb8-4fba-8f32-b8f388bf5bcc/
[h] https://cmip-publications.llnl.gov/view/CMIP6/?type=model&option=MPI-ESM1-2-LR
[i] https://cds.climate.copernicus.eu/cdsapp#!/dataset/projections-cordex-domains-single-levels?tab=overview

## Bibliografia

[1] Assessment of climate impact on grape productivity: A new application for bioclimatic indices in Italy, Massano et al. 2023

[2] Consequences of climate change on the tree of life in Europe, Thuiller et al. 2011

[3] Warming climate is helping human beings run faster, jump higher and throw farther through less dense air, Wang et al. 2024

[4] Impact of global changes on mountains, Grover et al. 2015

[5] Effect of multifunctional irrigation on grape quality: a case study in Northern Italy, Bianchi et al. 2023

[6] The geographical range of British birds expands during 15 years of warming, Massimino et al. 2015

[7] Effects of climate change on gilthead seabream aquaculture in the Mediterranean, Haberle et al. 2023

[8] Nidificazione del Gruccione (*Merops apiaster*) in ambiente montano, Cattaneo et al. 2019

[9] A Warm Welcome to the Alps—The Northward Expansion of Trithemis annulata (Odonata, Libellulidae) in Italy, La Porta et al. 2024

[10] Biodiversity stabilizes primary productivity through compensatory effects under warming conditions, Li et al. 2022

[11] Conservation of Mountain Biodiversity in the Context of Climate Change, Körner et al. 2009

[12] Bell-shaped tree-ring responses to air temperature drive productivity trends in long-lived mountain Mediterranean pines, Piovesan et al. 2023
[13] The CNRM-CM5.1 global climate model: description and basic evaluation (Voldoire et. Al 2012)
[14] Climate and carbon cycle changes from 1850 to 2100 in MPI-ESM simulations for the Coupled Model Intercomparison Project phase 5 (Giorgetta et al. 2013)
[15] Climate Change 2014 Synthesis Report, IPCC
[16] IPCC, 2019: Summary for Policymakers
[17] Climate System, Jost-Diedrich Graf Von Hardenberg, Politecnico di Torino
[18] Snow and Glacier Hydrology, Sigh et al. 2001
[19] Positive degree-day sums in the Alps: a direct link between glacier melt and international climate policy, Braithwhite et al. 2022